Deep-Sea Research I 58 (2011) 898–914

Contents lists available at ScienceDirect

Deep-Sea Research I

journal homepage: www.elsevier.com/locate/dsri

Particle fluxes in San Pedro Basin, California: A four-year record of sedimentation and physical forcing

Lisa E. Collins [a,b,*], William Berelson [b], Douglas E. Hammond [b], Angela Knapp [b,c], Richard Schwartz [b], Doug Capone [d]

[a] University of Southern California, Environmental Studies Program, 3502 Trousdale Pkwy SOS B15, Los Angeles, CA 90089-0036, USA
[b] University of Southern California, Earth Sciences, 3651 Trousdale Pkwy ZHS, Los Angeles, CA 90089-0740, USA
[c] University of Miami, Marine and Atmospheric Chemistry, 4600 Rickenbacker Causeway, Miami, FL 3314, USA
[d] University of Southern California, Marine Environmental Biology, 3616 Trousdale Pkwy AHF, Los Angeles, CA 90089, USA

ARTICLE INFO

Article history:
Received 6 November 2010
Received in revised form
11 May 2011
Accepted 23 June 2011
Available online 30 June 2011

Keywords:
Ocean carbon cycle
Remineralization
Organic carbon
Biogenic silica
San Pedro Basin
Sediment traps

ABSTRACT

Moored sediment traps were deployed from January 2004 through December 2007 at depths of 550 and 800 m in San Pedro Basin (SPB), CA (33°33.0′N, 118°26.5′W). Additionally, floating sediment traps were deployed at 100 and 200 m for periods of 12–24 h during spring 2005, fall 2007, and spring 2008. Average annual fluxes of mass, particulate organic carbon (POC), $\delta^{13}C_{org}$, particulate organic nitrogen (PON), δ^{15}N-PON, biogenic silica ($bSiO_2$), calcium carbonate ($CaCO_3$), and detrital material (non-biogenic) were coupled with climate records and used to examine sedimentation patterns, vertical flux variability, and organic matter sources to this coastal region. Annual average flux values were determined by binning data by month and averaging the monthly averages. The average annual fluxes to 550 m were 516 ± 42 mg/m^2 d for mass (sdom of the monthly averages, $n=117$), 3.18 ± 0.26 mmol C/m^2 d for POC ($n=111$), 0.70 ± 0.05 mmol/m^2 d for $CaCO_3$ ($n=110$), 1.31 ± 0.21 mmol/m^2 d for $bSiO_2$ ($n=115$), and 0.35 ± 0.03 mmol/m^2 d for PON ($n=111$). Fluxes to 800 and to 550 m were similar, within 10%. Annual average values of $\delta^{13}C_{org}$ at 550 m were -21.8 ± 0.2‰ ($n=108$), and δ^{15}N averages were 8.9 ± 0.2‰ ($n=95$). The timing of both high and low flux particle collection was synchronous between the two traps. Given the frequency of trap cup rotation (4–11 days), this argues for particle settling rates ≥ 83 m/d for both high and low flux periods. The moored traps were deployed over one of the wettest (2004–2005, 74.6 cm rainfall) and driest (2006–2007, 6.6 cm) rain years on record. There was poor correlation (Pearson's correlation coefficient, 95% confidence interval) of detrital mass flux with: C_{org}/N ratio ($r=0.10$, $p=0.16$); δ^{15}N ($r=-0.19$, $p=0.02$); and rainfall ($r=0.5$, $p=0.43$), suggesting that runoff does not immediately cause increases in particle fluxes 15 km offshore. $\delta^{13}C_{org}$ values suggest that most POC falling to the basin floor is marine derived. Coherence between satellite-derived chlorophyll *a* records from the trap location (± 9 km^2 resolution) and SST data indicates that productivity and export occurs within a few days of upwelling and both of these parameters are reasonable predictors of POC export, with a time lag of a few days to 2 weeks (with no time lag—SeaWiFS chlorophyll *a* and POC flux, $r=0.25$, $p=0.0014$; chlorophyll *a* and $bSiO_2$ flux, $r=0.28$, $p=0.0002$).

1. Introduction/background

The use of sediment traps moored to the seafloor has been a common technique for determining the magnitude and temporal patterns of particle fluxes in various oceanographic regimes (Honjo et al., 2008). Several sediment trap studies have been conducted in the Southern California borderland region (Fig. 1) over the last three decades to constrain the vertical flux of biogenic and detrital material in this coastal environment (Altabet et al., 1999; Bruland et al., 1981; Crisp et al., 1979; Dymond et al., 1981; Huh and Beasley, 1987; Huh et al., 1990; Huh et al., 1993; Moore et al., 1981; Nelson et al., 1987; Passow et al., 2001; Shipe and Brzezinski, 2001; Shipe et al., 2002; Thunell et al., 1999; Thunell, 1998; Thunell et al., 1994a; Thunell et al., 1994b). Of the aforementioned studies, the ones that were conducted in San Pedro Basin either captured no more than 6 months of sedimentation at high temporal resolution or captured longer intervals at very low temporal resolution. Santa Barbara Basin has been well studied at high resolution for several years through the use of both sediment traps and water column sampling. These studies (Passow et al., 2001; Shipe and Brzezinski, 2001; Shipe et al., 2002) have found significant couplings between ocean export of biogenic material and distal and local forcing (El Niño and upwelling). One question we

* Corresponding author at: University of Southern California, Environmental Studies Program, 3502 Trousdale Pkwy SOS B15, Los Angeles, CA 90089-0036, USA.
E-mail address: lecollin@usc.edu (L.E. Collins).

0967-0637/$ - see front matter © 2011 Elsevier Ltd. All rights reserved.
doi:10.1016/j.dsr.2011.06.008

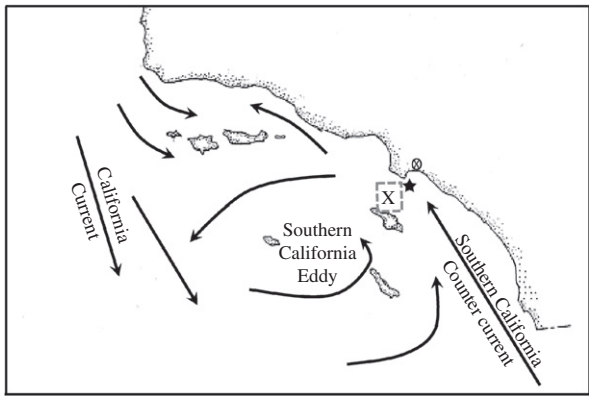

Fig. 1. Map view of the Southern California Bight, showing locations of the sediment trap—the San Pedro Ocean Time series—SPOT (X), and sea surface temperature NOAA buoy 46222 (star). The gray dashed boxes show the area integrated for SeaWiFS chlorophyll data at SPOT (around the X). Wind and rainfall data came from Long Beach (x with circle around it). Ocean and current information from B. Hickey, 1992.

address is whether the close coupling between climate forcing and sediment export, which results in varved laminations in Santa Barbara Basin, is comparable to the forcing and sedimentation, which does not produce varved sediments in San Pedro Basin.

Carbon export in continental margin environments is important to the global carbon cycle (Muller-Karger et al., 2005; Reimers et al., 1992; Thunell et al., 2007). In spite of coastal waters' relatively small contribution to the total area of the oceans, it is estimated that 40% of the carbon exported below the thermocline and to the seafloor occurs along continental margins (Muller-Karger et al., 2005). Currently, many global numerical models do not account for margins because of the small area relative to the entire ocean and their complex oceanography (Muller-Karger et al., 2005). Understanding the controls on the formation and export of particles in coastal regions will help better constrain global models and budgets for carbon, silica, and other elements.

One of the driving factors behind studies of marine carbon export is to describe and predict the remineralization rate of organic carbon. A commonly used formulation for the remineralization of organic carbon, described by Martin et al. (1987) is

$$F_z = F_{100\,\mathrm{m}}(z/100)^{-b} \quad (1)$$

which relates the flux of organic carbon to depth z, to the flux of organic carbon at 100 m. The exponent b changes the shape of flux attenuation such that larger b values mean more remineralization between 100 m and deeper waters and smaller b values result in less remineralization and a larger percentage of organic carbon exported to the deep ocean. It has been demonstrated that b varies regionally (Berelson, 2001; Devol and Hartnett, 2001; Buesseler et al., 2007a) and seasonally (Lohrenz et al., 1992), and thus the use of a single b value for the Martin equation may not be applicable globally. A mechanistic understanding of POC flux versus depth and the relevance of the b value remains a topic of discussion (Primeau, 2006; Buesseler, 1998; Buesseler et al., 2007b). Our work attempts to specifically examine the impact of physical forcing and understand the mechanisms determining mass flux and carbon export in an upwelling-dominated, continental margin system.

Here we document a 4-year, sediment trap time-series study from San Pedro Basin, offshore from Los Angeles, CA, referred to as SPOT (San Pedro Ocean Time series). This trap data complements other studies at this location including monthly water column measurements, which have provided the basis for a study of seasonal bacterial community change (Fuhrman et al., 2006) and documentation of domoic acid (DA) fluxes closely associated with DA appearance in the surface ocean (Schnetzer et al., 2007; Sekula-Wood et al. 2009). From traps deployed at 550 and 800 m we have generated a record of fluxes of POC, total carbon, nitrogen, bacterial C, $bSiO_2$, $CaCO_3$ as well as $\delta^{13}C_{total}$, $\delta^{13}C_{org}$, and $\delta^{15}N$ values of sedimenting material. Sources of POC, the difference in flux between 550 and 800 m, the relative timing of detrital and biogenic fluxes with respect to climatic forcing, and the remineralization pattern of POC with depth are discussed with the intent of better defining POC export processes in continental margin settings.

2. Study area

The Southern California Bight is characterized by its unique borderland morphology with many basins and islands/ridges (Fig. 1). Located between Los Angeles and Santa Catalina Island, San Pedro Basin (SPB) is one of the inner basins, bordered on the north/northwest by Santa Monica Basin. SPB is silled to the SE at a depth of ~740 m, and the basin water is suboxic, with bottom water oxygen ranging between 2 and 10 μM. Episodic flushing of the basin bottom waters (>750 m) occurs an average of every 12–24 months (Berelson, 1991; Hickey, 1991), and the maximum depth of the basin is 900 m.

The Bight is broadly influenced by the California Current system. The California Current moves south–southeast, offshore from SPB, and is better developed in the spring and early summer. As the California Current moves past Pt. Conception, some water splays into the southern portion of the Bight near San Clemente Island, and can turn north, creating a counter-clockwise rotating Southern California Eddy. At some times of the year, a countercurrent flows north, bringing warmer subtropical waters into the Bight (Wickham, 1975; Wooster and Reid, 1963). This occurs most often in the fall and winter, and the countercurrent is weak or non-existent in the spring (Hickey et al., 2003). Interactions of winds and surface currents with the morphology and bathymetry of the Southern California Bight create small cyclonic eddies, which interact with Catalina Island and Palos Verdes Peninsula (Dong and McWilliams, 2007). Water movement within the basin is not quiescent, even below the sill. Currents at 100 m average ~10 cm/s and decrease to ~0.5–1.0 cm/s below the sill at 800 m (Hickey, 1991). Thus, particles forming at the surface will be subjected to advection and dispersion both during their sinking from the upper ocean but also while settling through deeper waters. The assumption of 'vertical fluxes' will be tested in this manuscript.

3. Methods

3.1. Field sampling

Two McLane Mark V sediment traps (Honjo and Doherty, 1988) were moored in SPB (33°33.0′N and 118°30.0′W, Fig. 1) from January 2004 through December 2007, sampling continuously except when out of the water for mooring turn-around or when the traps clogged (denoted by (c) in Table 1). One trap was moored at 550 m (A trap) and the second at 800 m (B trap). After the first 10 months of deployment, we found that the deeper trap clogged frequently and an interior sleeve was added to decrease the collection area from 0.50 to 0.25 m^2. This area-restrictor remained in place for the remainder of the measurement period. Below the funnel of each trap a rotating carousel equipped with 21 cups (250 mL) open to the funnel for a variable (programmable) duration (typically 7 days). On a few occasions, a coastal model of this trap was used with a larger throat opening and 13 sampling cups. This trap never clogged. Trap solution was made from 0.2 μm-filtered seawater from the corresponding trap depth,

Table 1

ID	Date	Julian day	Mass (mg/m^2 d)	Mass ($\pm$)	$bSiO_2$ ($mmol/m^2$ d)	detrital (mg/m^2 d)	POC ($mmol/m^2$ d)	PON ($mmol/m^2$ d)	C_{org}/N	$CaCO_3$ ($mmol/m^2$ d)
A1-1	11/01/2004	11	225	33	0.47	110	1.60	0.17	9.4	0.29
A1-2	17/01/2004	17	483	10	0.89	287	2.49	0.24	10.2	0.49
A1-3	23/01/2004	23	450	3	0.86	272	2.05	0.19	10.6	0.47
A1-4	29/01/2004	29	525	6	1.19	290	2.58	0.26	10.0	0.63
A1-5	04/02/2004	35	287	4	0.64	153	1.54	0.16	9.6	0.36
A1-6	10/02/2004	41	454	5	1.10	224	2.63	0.26	10.0	0.63
A1-7	16/02/2004	47	644	12	1.85	275	3.90	0.38	10.3	1.04
A1-8	22/02/2004	53	1103	19	2.56	545	–	–	–	–
A1-9	28/02/2004	59	1096	6	2.43	661	5.00	0.50	10.0	0.90
A1-10	05/03/2004	65	644	6	1.19	385	3.38	0.36	9.3	0.61
A1-11	11/03/2004	71	1092	14	2.65	516	6.01	0.57	10.5	1.83
A1-12	17/03/2004	77	641	11	1.47	299	3.64	0.36	10.0	1.14
A1-13	23/03/2004	83	304	3	0.76	142	1.68	0.18	9.6	0.49
A1-14	29/03/2004	89	95	5	0.22	38	–	–	–	–
A1-15	04/04/2004	95	290	2	0.83	122	2.32	0.25	9.5	0.30
A1-16	10/04/2004	101	211	7	0.81	75	1.99	0.22	8.9	0.11
A1-17 (c)	16/04/2004	107	63	1	–	–	–	–	–	–
B1-1	11/01/2004	11	246	13	0.37	159	1.26	0.11	11.1	0.18
B1-2	17/01/2004	17	486	8	0.75	311	2.27	0.20	11.5	0.46
B1-3	23/01/2004	23	696	22	1.42	439	2.83	0.25	11.2	0.58
B1-4	29/01/2004	29	701	3	1.52	396	3.05	0.30	10.7	0.92
B1-5	04/02/2004	35	383	9	0.74	–	1.74	0.16	11.1	0.37
B1-6	10/02/2004	41	518	3	1.00	306	2.41	0.22	10.8	0.59
B1-7	16/02/2004	47	817	15	1.74	461	3.83	0.36	10.8	1.02
B1-8	22/02/2004	53	1160	9	2.91	753	5.91	0.40	–	–
B1-9 (c)	28/02/2004	59	1864	27	3.83	883	7.65	1.03	7.4	4.41
A2-1	16/06/2004	168	287	14	0.71	99	1.82	0.12	–	0.78
A2-2	23/06/2004	175	353	13	0.57	95	2.41	0.32	7.5	1.37
A2-3	30/06/2004	182	338	7	0.61	46	2.70	–	–	–
A2-4	07/07/2004	189	179	12	0.41	0	–	–	–	–
A2-5	14/07/2004	196	252	6	0.56	106	2.36	0.23	10.2	0.28
A2-6	21/07/2004	203	342	4	0.93	149	3.44	0.32	10.8	0.13
A2-7	28/07/2004	210	371	8	0.86	78	3.71	0.42	10.5	1.08
A2-8	04/08/2004	217	437	25	1.14	97	3.82	0.42	9.2	1.33
A2-9	11/08/2004	224	359	5	0.87	144	2.35	0.28	8.5	0.74
A2-10	18/08/2004	231	272	3	0.76	68	2.14	0.26	11.1	0.77
A2-11	25/08/2004	238	–	–	–	–	–	–	–	–
A2-12	01/09/2004	245	806	31	1.13	423	4.89	0.56	8.8	1.40
A2-13	08/09/2004	252	519	5	0.72	260	2.96	0.31	9.5	1.10
A2-14	15/09/2004	259	921	13	1.08	587	4.31	0.42	10.2	1.25
A2-15	22/09/2004	266	397	11	0.65	211	2.15	0.23	9.4	0.68
A2-16	29/09/2004	273	317	7	0.49	180	1.77	0.19	9.3	0.43
A2-17	06/10/2004	280	199	11	0.35	100	1.23	0.14	9.0	0.32
A2-18	13/10/2004	287	520	10	0.92	279	3.06	0.34	9.1	0.73
A2-19	20/10/2004	294	555	4	0.96	314	3.19	0.33	9.8	0.66
A2-20 (c)	27/10/2004	301	317	6	0.47	175	2.05	0.25	8.2	0.41
A3-1	14/12/2004	349	848	9	1.13	536	4.16	0.46	9.1	0.93
A3-2	21/12/2004	356	582	55	0.76	380	2.75	0.29	9.2	0.56
A3-3	28/12/2004	363	292	8	0.45	166	1.64	0.19	8.6	0.39
A3-4	04/01/2005	370	543	37	0.57	381	1.91	0.21	9.0	0.58
A3-5	11/01/2005	377	333	88	0.36	187	1.51	0.19	7.9	0.70
A3-6	18/01/2005	384	869	74	0.90	660	3.43	0.37	9.3	0.31
A3-7	25/01/2005	391	612	28	0.77	421	2.47	0.27	9.3	0.53
A3-8	01/02/2005	398	422	46	0.67	260	1.90	0.22	8.8	0.49
A3-9	08/02/2005	405	384	46	0.49	247	1.57	0.20	8.0	0.48
A3-10	15/02/2005	412	471	38	0.68	311	1.84	0.20	9.3	0.49
A3-11	22/02/2005	419	903	29	1.25	624	3.20	0.34	9.4	0.82
A3-12	01/03/2005	426	737	21	0.99	508	2.67	0.29	9.2	0.67
A3-13	08/03/2005	433	642	10	0.99	415	2.91	0.31	9.3	0.59
A3-14	15/03/2005	440	711	36	1.18	437	3.13	0.33	9.5	0.83
A3-15	22/03/2005	447	581	17	1.28	359	3.42	0.36	9.3	0.15
A3-16	29/03/2005	454	782	7	2.78	353	4.69	0.50	9.4	0.66
A3-17	05/04/2005	461	1386	21	6.30	435	8.66	0.92	9.5	1.91
A3-18	12/04/2005	468	2088	39	8.42	938	10.94	1.26	7.6	1.54
A3-19 (c)	19/04/2005	475	787	15	3.50	310	4.54	0.56	8.2	0.63
B3-1	14/12/2004	349	602	73	0.84	373	2.92	0.31	9.4	0.72
B3-2	21/12/2004	356	558	64	0.72	360	2.56	0.26	9.7	0.62
B3-3	28/12/2004	363	382	33	0.52	242	–	–	–	–
B3-4	04/01/2005	370	715	94	0.75	497	2.63	0.29	9.2	0.76
B3-5	11/01/2005	377	408	90	0.48	273	1.64	0.18	8.9	0.45
B3-6	18/01/2005	384	706	158	0.75	501	2.76	0.29	9.6	0.59
B3-7	25/01/2005	391	485	39	0.56	340	1.92	0.20	9.5	0.41
B3-8	01/02/2005	398	342	23	0.47	227	1.39	0.15	9.3	0.35

Table 1 (*continued*)

ID	Date	Julian day	Mass (mg/m^2 d)	Mass (±)	bSiO$_2$ (mmol/m^2 d)	detrital (mg/m^2 d)	POC (mmol/m^2 d)	PON (mmol/m^2 d)	C_{org}/N	$CaCO_3$ (mmol/m^2 d)
B3-9	08/02/2005	405	541	42	0.68	373	1.95	0.20	9.6	0.54
B3-10	15/02/2005	412	529	104	0.64	360	2.04	0.21	9.6	0.55
B3-11	22/02/2005	419	577	28	0.80	306	0.77	0.21	–	1.83
B3-12	01/03/2005	426	677	60	0.92	472	2.49	0.26	9.5	0.56
B3-13	08/03/2005	433	467	53	0.69	316	–	–	–	–
B3-14	15/03/2005	440	504	38	0.87	315	2.30	0.25	9.1	0.49
B3-15	22/03/2005	447	474	25	1.13	251	2.85	0.31	9.3	0.46
B3-16	29/03/2005	454	782	57	2.56	378	4.34	0.46	9.5	0.70
B3–17	05/04/2005	461	1562	66	6.36	667	9.24	0.94	9.9	1.13
B3-18	12/04/2005	468	2035	63	7.84	933	10.76	1.21	8.9	1.57
B3-19 (c)	19/04/2005	475	1441	19	6.14	538	–	–	–	–
A4-1	20/05/2005	506	577	13	1.43	276	3.54	0.42	8.5	0.69
A4-2	26/05/2005	512	732	25	2.18	301	5.22	0.60	8.7	0.86
A4-3 (c)	01/06/2005	518	245	8	1.01	47	2.50	0.29	8.7	0.34
B4-1	20/05/2005	506	602	17	1.47	312	3.24	0.37	8.7	0.61
B4-2	26/05/2005	512	972	25	3.22	413	6.27	0.71	9.0	0.95
B4-3 (c)	01/06/2005	518	658	14	2.39	201	5.58	0.65	8.5	0.81
A5-1	05/10/2005	644	848	11	1.61	325	9.66	1.12	8.6	0.91
A5-2	13/10/2005	652	840	16	1.22	482	5.66	0.67	8.7	0.83
A5-3	21/10/2005	660	708	14	0.99	438	4.20	0.42	9.9	0.61
A5-4 (c)	29/10/2005	668	359	21	0.49	183	3.69	0.51	7.3	0.19
B5-1	05/10/2005	644	1047	16	–	–	8.62	0.85	10.2	0.89
B5-2	13/10/2005	652	790	7	1.16	467	5.56	0.65	8.4	0.56
B5-3	21/10/2005	660	623	15	0.97	369	3.63	0.40	9.3	0.64
B5-4 (c)	29/10/2005	668	297	17	0.39	155	2.94	0.42	6.9	0.17
A6-1	31/03/2006	824	396	5	2.16	90	2.84	0.31	9.1	0.57
A6-2	08/04/2006	832	360	9	1.91	29	–	0.47	–	–
A6-3	16/04/2006	840	775	7	4.23	181	6.07	0.70	8.7	0.82
A6-4	24/04/2006	848	631	19	3.60	99	6.30	0.75	8.2	0.65
A6-5	02/05/2006	856	709	3	2.90	157	8.56	0.81	10.4	0.73
A6-6	10/05/2006	864	195	5	0.74	40	2.33	0.26	8.8	0.25
A6-7	18/05/2006	872	188	1	0.58	40	2.20	0.25	8.6	0.37
A6-8	26/05/2006	880	318	3	0.81	56	2.75	0.44	6.3	1.09
A6-9	03/06/2006	888	369	5	0.93	163	3.22	0.32	10.1	0.38
A6-10	11/06/2006	896	242	4	0.55	117	2.09	0.21	10.0	0.16
A6-11	19/06/2006	904	159	3	0.34	60	1.56	0.18	9.7	0.26
A6-12	27/06/2006	912	252	3	0.64	94	2.21	0.23	8.7	0.39
A6-13	05/07/2006	920	628	8	2.08	210	5.24	0.55	9.4	0.92
B6-1	31/03/2006	824	664	18	3.83	185	4.73	0.49	9.6	0.34
B6-2	05/04/2006	829	979	8	5.20	329	6.39	0.65	9.8	0.49
B6-3	10/04/2006	834	567	10	2.98	185	4.14	0.41	10.1	0.23
B6-4	15/04/2006	839	809	2	4.32	246	6.97	0.67	10.4	0.11
B6-5	20/04/2006	844	1042	5	5.18	394	7.19	0.69	10.5	0.23
B6-6	25/04/2006	849	1164	19	7.16	258	8.67	0.89	9.7	0.95
B6-7	30/04/2006	854	612	12	2.67	232	5.41	0.58	9.3	0.03
B6-8	05/05/2006	859	720	13	3.19	134	8.19	0.74	11.0	0.96
B6-9	10/05/2006	864	313	17	1.24	80	3.30	0.33	10.1	0.36
B6-10	15/05/2006	869	226	4	0.83	72	2.08	0.21	9.8	0.25
B6-11	20/05/2006	874	155	5	0.49	75	1.18	0.11	11.2	0.06
B6-12	25/05/2006	879	242	31	–	–	1.82	0.16	11.5	0.07
B6-13	30/05/2006	884	382	11	0.95	208	3.00	0.27	11.2	0.07
B6-14	04/06/2006	889	407	16	1.07	210	3.50	0.30	11.7	0.04
B6-15	09/06/2006	894	465	3	1.07	235	3.53	0.33	10.1	0.40
B6-16	14/06/2006	899	265	8	0.62	–	2.05	–	–	–
B6-17	19/06/2006	904	361	16	0.75	210	2.45	0.21	11.4	0.17
B6-18	24/06/2006	909	230	13	0.55	121	1.85	0.16	11.3	0.08
B6-19	29/06/2006	914	207	3	0.57	85	1.72	0.16	10.5	0.27
B6-20	04/07/2006	919	518	11	1.68	228	4.37	0.39	11.2	0.23
B6-21	09/07/2006	924	755	20	2.33	360	6.32	0.53	11.9	0.18
B7-1	13/08/2006	956	295	25	0.52	181	1.79	0.14	12.5	0.20
B7-2	20/08/2006	963	570	108	0.84	365	3.37	0.28	12.1	0.36
B7-3	27/08/2006	970	708	148	1.02	471	4.00	0.33	12.2	0.33
B7-4	03/09/2006	977	418	5	0.67	273	2.48	0.20	12.3	0.17
B7-5	10/09/2006	984	465	12	0.78	298	2.96	0.23	12.7	0.15
B7-6 (c)	17/09/2006	991	252	10	0.41	161	1.65	0.16	10.5	0.07
A8-1	19/01/2007	1115	615	14	1.40	351	2.53	0.26	9.6	0.78
A8-2	29/01/2007	1125	1144	25	6.13	347	6.528	0.75	8.7	1.18
A8-3	03/02/2007	1130	973	30	4.49	345	5.548	0.66	8.4	1.06
A8-4	07/02/2007	1134	579	18	2.09	252	2.98	0.35	8.6	0.71
A8-5	11/02/2007	1138	286	9	1.04	103	1.71	0.21	8.1	0.48

Table 1 (*continued*)

ID	Date	Julian day	Mass (mg/m^2 d)	Mass (±)	$bSiO_2$ ($mmol/m^2$ d)	detrital (mg/m^2 d)	POC ($mmol/m^2$ d)	PON ($mmol/m^2$ d)	C_{org}/N	$CaCO_3$ ($mmol/m^2$ d)
A8-6	15/02/2007	1142	248	9	0.99	82	1.59	0.19	8.2	0.38
A8-7	19/02/2007	1146	341	13	1.01	148	1.86	0.24	7.7	0.55
A8-8	23/02/2007	1150	360	9	0.83	193	1.62	0.19	8.4	0.51
A8-9	27/02/2007	1154	209	5	0.43	112	1.13	0.16	7.3	0.28
A8-10	03/03/2007	1158	317	10	0.61	176	1.61	0.22	7.2	0.42
A8-11	07/03/2007	1162	145	3	0.38	69	1.02	0.14	7.1	0.14
A8-12	11/03/2007	1166	584	18	1.78	279	2.99	0.38	7.9	0.73
A8-13	15/03/2007	1170	1357	52	4.56	682	6.88	0.75	9.1	1.05
A8-14	19/03/2007	1174	2730	65	10.41	1207	13.94	1.56	8.9	2.79
A8-15	23/03/2007	1178	2273	20	6.62	1199	10.18	1.16	8.7	2.40
A8-16	27/03/2007	1182	617	24	1.52	333	2.74	0.31	8.8	0.79
A8-17	31/03/2007	1186	366	9	0.90	152	2.00	0.28	7.0	0.79
A8-18	04/04/2007	1190	564	6	1.28	216	3.54	0.45	7.9	1.36
A8-19	08/04/2007	1194	721	19	1.55	290	4.15	0.51	8.1	1.79
A8-20	12/04/2007	1198	459	18	1.13	171	2.67	0.33	8.0	1.15
A8-21	16/04/2007	1202	340	30	–	–	–	0.23	8.2	–
B8-1	19/01/2007	1115	475	29	0.85	294	2.10	0.23	9.0	0.49
B8-2	29/01/2007	1125	1591	29	7.40	569	8.39	0.97	8.6	1.84
B8-3	04/02/2007	1131	972	22	4.13	394	4.95	0.54	9.1	1.03
B8-4	10/02/2007	1137	594	19	2.15	263	2.84	0.32	9.0	0.75
B8-5	16/02/2007	1143	487	11	1.55	229	2.32	0.25	9.3	0.66
B8-6	22/02/2007	1149	503	11	1.38	261	2.32	0.25	9.1	0.62
B8-7	28/02/2007	1155	514	26	1.32	258	–	0.33	–	0.68
B8-8	06/03/2007	1161	321	6	0.92	147	1.70	0.21	7.9	0.49
B8-9	12/03/2007	1167	945	5	3.62	421	4.97	0.58	8.6	0.87
B8-10	18/03/2007	1173	2130	86	7.66	937	10.78	1.29	8.2	2.60
B8-11	24/03/2007	1179	1123	26	3.83	496	5.71	0.66	8.6	1.51
B8-12	30/03/2007	1185	220	7	0.60	86	1.34	0.20	6.8	0.45
B8-13	06/04/2007	1192	354	16	0.74	161	2.46	0.31	7.9	0.57
B8-14	12/04/2007	1198	297	12	0.56	126	2.16	0.27	7.9	0.59
B8-15	18/04/2007	1204	200	10	0.37	85	0.96	0.15	6.6	0.55
B8-16	24/04/2007	1210	768	20	3.45	276	4.07	0.46	8.8	0.98
B8-17	30/04/2007	1216	1516	20	6.52	327	7.78	1.35	5.8	4.32
B8-18	06/05/2007	1222	1086	37	6.61	229	11.04	1.09	10.1	–
B8-19	12/05/2007	1228	231	7	1.23	12	1.44	0.22	6.5	0.77
B8-20	18/05/2007	1234	336	11	1.32	134	2.66	0.26	10.2	0.16
B8-21	24/05/2007	1240	100	9	0.36	15	1.16	0.19	6.0	0.20
A9-1	03/07/2007	1280	672	7	2.31	266	3.79	0.43	8.7	1.09
A9-2	11/07/2007	1288	628	6	2.38	202	3.99	0.46	8.6	1.15
A9-3	19/07/2007	1296	524	7	2.37	153	3.56	0.39	9.0	0.75
A9-4	27/07/2007	1304	588	16	2.04	180	3.77	0.47	8.0	1.31
A9-5	04/08/2007	1312	298	6	0.77	110	2.06	0.25	8.1	0.63
A9-6	12/08/2007	1320	566	15	1.15	299	3.17	0.36	8.7	0.78
A9-7	20/08/2007	1328	608	10	1.03	344	3.49	0.42	8.3	0.73
A9-8	28/08/2007	1336	332	11	0.85	138	1.90	0.26	7.2	0.54
A9-9	05/09/2007	1344	290	13	0.87	104	2.22	0.25	9.0	0.49
A9-10	13/09/2007	1352	496	11	1.96	146	3.78	0.45	8.3	0.79
A9-11	21/09/2007	1360	365	104	1.38	116	2.84	0.35	8.2	0.52
A9-12	29/09/2007	1368	133	2	0.34	49	1.00	0.13	8.0	0.26
A9-13	07/10/2007	1376	124	3	0.27	45	0.93	0.10	9.0	0.28
A9-14	15/10/2007	1384	445	8	0.63	254	2.28	0.24	9.7	0.71
A9-15	23/10/2007	1392	538	2	0.99	284	3.05	0.30	10.0	0.82
A9-16	31/10/2007	1400	637	4	1.32	340	3.57	0.35	10.3	0.82
A9-17	08/11/2007	1408	590	23	0.76	391	2.50	0.27	9.8	0.60
A9-18	16/11/2007	1416	555	27	0.64	371	2.52	0.27	8.0	0.55
A9-19	24/11/2007	1424	474	16	0.66	300	2.27	0.24	9.1	0.52
A9-20	02/12/2007	1432	144	8	0.19	85	0.95	0.12	7.9	0.14
A9-21	10/12/2007	1440	81	6	0.13	31	0.78	0.14	5.8	0.13
B9-1	03/07/2007	1280	795	26	2.69	303	4.58	0.53	8.7	1.39
B9-2	11/07/2007	1288	506	19	1.97	153	3.41	0.40	8.4	0.93
B9-3	19/07/2007	1296	410	4	1.42	141	2.61	0.32	8.2	0.76

lD Sample ID—A is the trap at 550 m, B is the trap at 800 m. The first number indicates deployment #, the second indicates the cup #, i.e. B3-3 is trap B (800 m), deployment #3, cup #3.
Date The midpoint date that the cup was open, i.e., if cup was open for 7 days and rotated open on July 1, the date would be July 4.
Julian day January 1, 2004 is day 1 and we count sequentially up from that day.
Mass Mass from one split∗10 splits∗(1/trap area∗# days)=flux in mg/m^2 d.
Stdev Sample standard deviation of the mass flux. Each sample was split into 10, four splits were filtered, dried, and weighed to determine mass.
$bSiO_2$ Flux of biogenic silica (opal) in $mmol/m^2$ d where the molecular weight of $bSiO_2$ is 60.09 mg/mmole (wt% $bSiO_2$/100)∗mass flux.
Detrital Flux of all non-biogenic constituents, including water associated with opal and assuming organic matter molecular weight=30 g/mole.
POC Flux of organic carbon (%C acidified/100)∗mass flux∗(1 mmole/12 mg C).
C_{org}/N (%C_{org}/%N)∗(14/12).
$CaCO_3$ (%TIC/100)∗mass flux∗(1 mmol/100 mg $CaCO_3$).
Total C (%C/100)∗mass flux∗(1 mmole/12 mg C).
(c) indicates trap clogged so samples after clog are not reported as their flux is not reliable.

with salinity increased with NaCl by 5–6 ppt, formaldehyde added to a final concentration of 2%, and buffered with borate to pH=8 following JGOFS protocol (Knap, 1994). Upon trap recovery, samples were sealed and placed on ice for transport to the laboratory.

To collect settling particles from near the surface ocean, two free floating, surface tethered particle interceptor traps (PITs; Soutar et al., 1977) were deployed, one at 100 m and one at 200 m. One deployment was in May 2005 and seven deployments occurred between November 2007 and June 2008. The traps drifted to the NW with surface currents, typically a total of 12 ± 4 km over 24 h; satellite-tracking buoys continually monitored their position. The solution in these floating traps was 0.2 μm-filtered seawater from the corresponding trap depth with salinity increased by 10 ppt, borate buffered, and no additional preservatives. Upon recovery, samples were placed on ice until return to the lab where processing occurred immediately.

3.2. Sample processing and analysis

Sediment trap samples were stored at 4 °C until processed, which typically occurred within 1–3 days of trap recovery. Trap cups were shaken to homogenize the overlying liquid; an aliquot of this liquid was filtered and stored for nutrient analysis (dissolved Si as described below and phosphate, not discussed here). All solid cup material was passed through a 1000 μm sieve (JGOFS recommended procedure) to remove large particles, deemed 'swimmers'; >99% of the cup material passed through the 1000 μm sieve. By sieving trap material we may be inadvertently removing some particles that belonged in the flux category; however, our 4-year effort resulted in few amorphous particles removed on the sieve. Most of the particles >1000 μm were fish larvae or medusa of some sort, which we believe to have been 'swimmers'. Alternatively, some 'swimmers' may have passed through the sieve. If this processing approach affected results significantly, it might be expected to affect traps at the two depths differently. Material passing this screen was split into ten equal aliquots using a McLane rotary splitter. Four of these 10 splits were filtered onto separate 0.45 μm polycarbonate filters, rinsed 3 times with deionized water totaling a rinse volume of 10–15 mL, and dried at 25 °C until constant mass was reached (2 weeks or more). Sample weight reproducibility was ±5% among the four splits. Following weighing, material from three or four filters was combined, ground to homogenize, and the powdered sample was used to determine total carbon, total nitrogen, organic carbon, isotope values, and biogenic silica concentrations. Splits of this material were also used for radioisotope analysis.

3.3. Total carbon, total nitrogen, organic carbon, inorganic carbon flux and $\delta^{13}C$, $\delta^{15}N$ data

Weight %C and N were measured at USC on an Elantech 1110 Elemental Analyzer (EA). The standard used for C and N analysis was sulfanilamide (41.84 %C, 16.27 %N). A number of samples were also sent to UC Davis for analysis, and results for the two labs typically agreed within ±3% (ssd, relative precision). Organic carbon was measured at USC with the EA using an adapted method from Harris et al. (2001) in which inorganic carbon was removed by loading ~10 mg of sample into a silver cup, adding 50 μL of deionized water and placing samples in a dessicator with a beaker containing 30 mL of concentrated hydrochloric acid. After 8 h, the samples were removed and placed into a drying oven at 55 °C overnight. Reproducibility was established by analyzing a split of San Pedro Basin sediment; for nine runs of SPB sediments the total C precision was ±0.06 wt%, wt% C_{org} precision was ±0.06, and N precision was ±0.003 wt% (on a sample that contained 4.33 wt% C, 3.34 wt% C_{org}, and 0.40 wt% N). We applied these uncertainties to the wt% data presented here.

Wt% particulate inorganic carbon (PIC) was determined as the difference between acidified and un-acidified sample splits analyzed by EA. $CaCO_3$ flux in molar units was determined as

$$CaCO_3 \text{flux} = [((\%\text{total C} - \%C_{org})/100) * \text{mass flux}]/12 \quad (2)$$

with factor 12 representing the molecular weight of C (g/mole).

Carbon isotopic values are reported using the standard convention:

$$\delta^{13}C_{totalC}(‰) = \{(^{13}C/^{12}C_{sample})/(^{13}C/^{12}C_{PDB}) - 1\} * 1000 \quad (3)$$

Analyses of $\delta^{13}C_{totalC}$ and $\delta^{15}N$ in ‰ versus atmospheric $N_2 = \{(^{15}N/^{14}N)_{sample}/(^{15}N/^{14}N)_{air} - 1\} * 1000$ were performed by the stable isotope facility at UC Davis on un-acidified samples. The $\delta^{13}C$ of organic carbon ($\delta^{13}C_{org}$) was calculated using a mass balance equation:

$$\delta^{13}C_{org} = \{\delta^{13}C_{totalC} - ((1 - f_{C_{org}}) * \delta^{13}C_{C_{inorg}})\}/f_{C_{org}} \quad (4)$$

where $\delta^{13}C_{totalC}$ was measured, $f_{C_{org}}$ is known from sample acidification and measurement on the EA, and $\delta^{13}C_{C_{inorg}}$ was assumed to be 1‰. The assumption that $\delta^{13}C_{C_{inorg}} = 1‰$ is reasonable, given values measured by Hagadorn et al. (1995) in Santa Monica Basin sediments; furthermore, $\delta^{13}C_{org}$ in not sensitive to small changes in $\delta^{13}C_{C_{inorg}}$. However, we note that this approach creates a potential to introduce a spurious correlation between $\delta^{13}C_{org}$ and C/N for organic material: error propagation based on Eq. (4) and the $(C/N)_{org}$ ratio shows that for these samples, random errors in the fraction of organic matter would create a correlation with a slope of about +2.0‰ if $\delta^{13}C_{org}$ is plotted versus the atomic C/N of organic matter. However, the mean $\delta^{13}C_{org}$ for all samples should not be affected by random errors in individual samples.

3.4. Silica

Solid phase biogenic silica (bSi or $bSiO_2$) was determined using a hot sodium bicarbonate leaching method (DeMaster, 1979; DeMaster, 1991; Strickland, 1968). In all, 10–15 mg of dry, powdered sediment was placed in a 50 mL plastic centrifuge tube and 45 mL of 5% (wt./vol.) sodium bicarbonate solution was added. The solution was incubated for 5 h at 80 °C in a water bath and samples were mixed periodically. Subsamples of 1 mL were collected after 3, 4, and 5 h, neutralized with dilute hydrochloric acid and analyzed colorimetrically. The dissolved Si content of this solution was plotted versus leach time and the *y*-axis intercept taken as the amount of Si released from $bSiO_2$. This molar quantity of Si was converted to g of SiO_2 and the wt% $bSiO_2$ in a sample was thus determined. Flux is reported as mmol bSi/m^2 d and the Si is assumed to be stoichiometrically SiO_2 with a molecular weight of 60.09 g/mole. Supernatant from the overlying cup solution was also analyzed and this quantity was factored into the final $bSiO_2$ value to account for small amounts of dissolution (<5%) that occurs in the cup between collection and sample processing.

3.5. Detrital or lithogenic fraction

The flux of detrital material at SPOT was determined by subtracting the biogenic fluxes from the total mass flux, and so includes clays and other continentally derived material often termed the lithogenic fraction. We formulated this calculation as

$$\%\text{detrital} = 100 - \%\text{organic carbon compounds} - \%CaCO_3 - \%bSiO_2 - \%\text{organic N} \quad (5)$$

Percent C_{org} was multiplied by 2.5 (approximately the molecular weight of organic CH_2O divided by the atomic weight of carbon) to convert $\%C_{org}$ to %organic carbon compounds. $\%CaCO_3$ was determined from %TIC by multiplying by 8.33, the ratio of molecular weights of $CaCO_3$ to C. The wt% $bSiO_2$ was multiplied by 1.12 to account for a hydrated biogenic Si composition as $SiO_2{*}0.4H_2O$ (Mortlock and Froelich, 1989). %N, as reported by EA analysis on un-acidified samples, was multiplied by 1.2 to account for organic N in the form of NH_3.

3.6. Bacterial quantification

Sediment trap samples collected in the first 1.5 years of deployments were processed to determine the number of bacteria associated with falling particles. One of ten splits was used for enumeration, following the protocols of Kepner and Pratt (1994). A subsample of a well-mixed split was diluted between 1:100 and 1:1000 with Milli-Q water in 0.01% sodium dodecyl sulfate and 10 mM sodium pyrophosphate. Samples were sonicated using a probe sonicator for 30 s, filtered onto 0.2 μm black polycarbonate filters and stained with Vectashield® mounting medium with 4′,6-diamidino-2-phenylindole (DAPI, Vector Laboratories, Burlingame, CA, USA). Counts were made on an Olympus BX60 epifluorescent microscope at 1000× magnification. At least ten fields were counted per slide (n=100–400 bacteria). Triplicate slide preparation showed reproducible counts to ±10%. Bacteria per gram sediment was determined by dividing the bacterial cells per filter by the dry sediment mass on the filter.

3.7. Pb-210

Replicate multicores were taken in January 2006, stored briefly, and sectioned. Each interval was dried at 60 °C to determine porosity, ground slightly, and then placed in a polyethylene tube (9 mm OD) for gamma counting in a well-type intrinsic Ge gamma counter (Ortec). Each interval was counted for approximately 2 days, on two occasions. One core was sectioned to about 20 cm, and a second to 2 cm. ^{210}Pb activity was determined from its 46 keV peak. The supported activity for each sample was determined from the activity of its progenitors, ^{214}Pb (298 and 352 keV) and ^{214}Bi (609 keV). A weighted average of these three peaks was computed and increased by 10% to account for ^{222}Rn loss. The ^{222}Rn loss has been determined based on directly measuring the loss from sediments that have been processed similarly. Instrument calibration was based on a diluted pitchblende EPA standard (SRM-DP2) in the same geometry. Uncertainties were determined from counting statistics. Self-absorption should be <3%, identical for the sediment samples and standard. Analyses have been decay corrected to the date of sample collection. The integrated mass of solids from the core top to the sample midpoint was computed based on porosity measurements. Sample weights were corrected for salt contribution (up to 20% for upper intervals), and the resulting profile was fit with an exponential function to obtain the sediment mass accumulation rate and inventory of ^{210}Pb in the profile (Fig. 2). Trap samples were also counted to determine excess ^{210}Pb activity and fluxes, obtained by multiplying the activity by the mass flux. Sample geometries varied slightly, depending on the available mass, and data was corrected for these differences. Data were binned by the month to obtain an annual average into each trap.

3.8. Climatological data

Rainfall, wind speed, and wind direction data (later two not reported here) were obtained from the National Climatic Data Center, Long Beach Daugherty Field station (www.ncdc.noaa.gov/), which is located near the study site (Fig. 1). Monthly chlorophyll

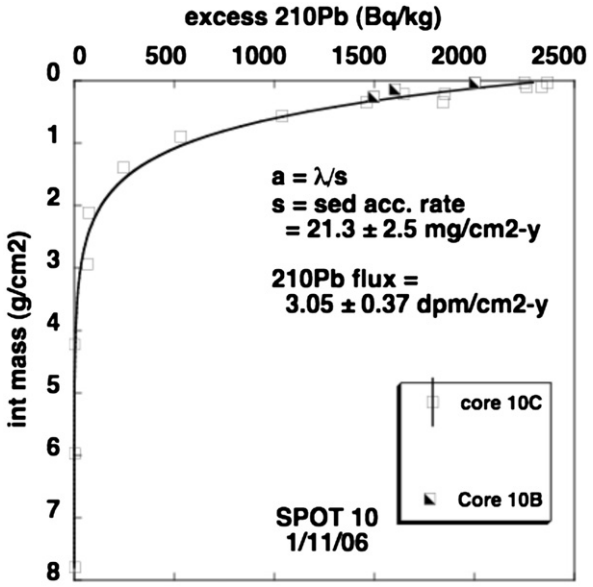

Fig. 2. Excess ^{210}Pb for two subcores (B and C) from a multi-core deployment plotted versus integrated density (providing accumulated mass). Results were in good agreement near the surface where both cores were counted. An exponential function was fit to the profiles. The integration of the fit produced results shown in the figure. Counting uncertainties for excess ^{210}Pb are slightly less than the size of the symbol.

data came from NASA's SeaWiFS satellite (http://reason.gsfc.nasa.gov/OPS/Giovanni/ocean.swf8D.2.shtml); the resolution of this data product was a 9 km × 9 km integrated area. We examined chlorophyll data for one grid north, south, east, and west of SPOT, saw generally good coherence, and chose to report the average chlorophyll for the entire area (27 km × 27 km) to cover a larger portion of the ocean potentially contributing particles to the trap location. Sea surface temperature data were downloaded from the National Oceanic and Atmospheric Administration (NOAA) buoy 46422, located in SPB (33°37′4″N and 118°19′1″W) ~7 km from SPOT. The buoy records temperature twice an hour. Temperatures for the upper 150 m of the water column were also obtained from the SPOT conductivity–temperature–depth (CTD) used on the monthly cruises. These temperatures were in close agreement with the NOAA buoy data, thus only buoy data is reported here, but is safely assumed to be representative of the trap location.

3.9. Statistical analysis

Linear correlation coefficients were calculated for parameters measured in the sediment traps to determine relationships between variables. Pearson's correlation coefficient (r) was calculated, and if it exceeded the 95% confidence interval, the strength of the linear relationship between variables was considered significant. The square of this value defines the fraction of the variance the relation explains. The stated p values indicate the probability that the correlation is not significant at this level. Two parameters with a correlation value yielding $p<0.05$ are considered significantly related.

4. Results

4.1. Magnitude and timing of fluxes in the 550 and 800 m deep-moored traps

The timing and magnitude of the fluxes between 550 and 800 m traps are highly correlated: mass (r=0.81, p=0.0001), POC

(r=0.87, p=0.0001), PON (r=0.86, p=0.0001), $CaCO_3$ (r=0.52, p=0.0001) and $bSiO_2$ (r=0.87, p=0.0001) (Figs. 3 and 4). However, many gaps in the 4-year record exist due to trap failures. All monthly average fluxes are reported in Table 2, and Table 3 reports the average monthly fluxes only when both the 550 m (A) and 800 m (B) trap collected, showing that the timing and

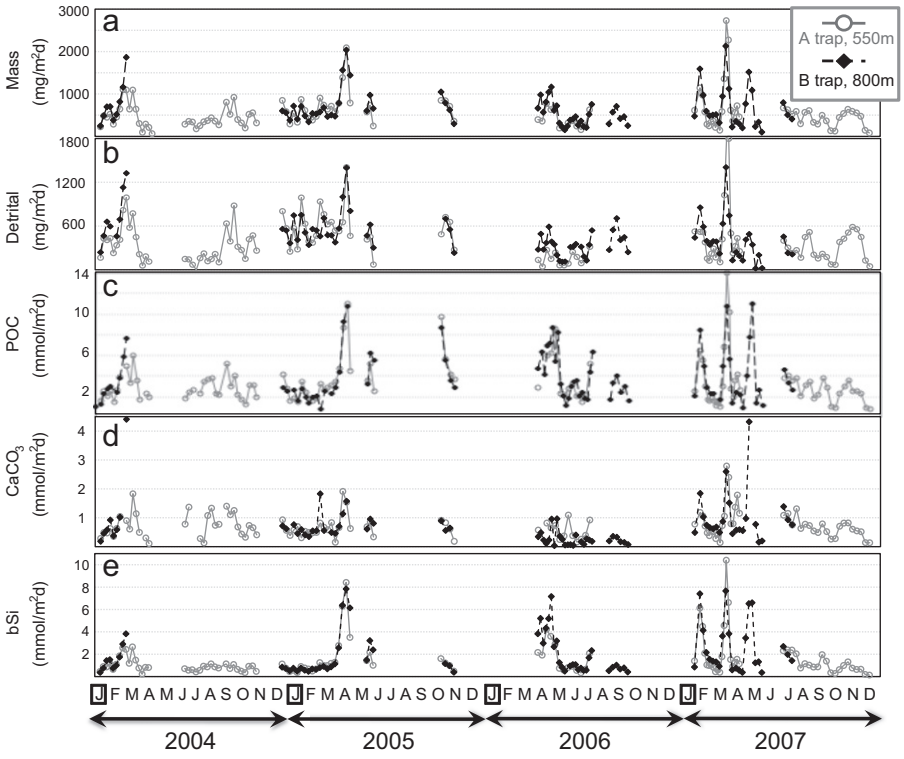

Fig. 3. (a) Mass flux (mg/m^2 d), (b) detrital (all non-biogenic flux) (mg/m^2 d), (c) particulate organic carbon flux (mmol/m^2 d), (d) calcium carbonate flux (mmol/m^2 d), (e) biogenic silica (mmol/m^2 d). All plots start January 1, 2004.

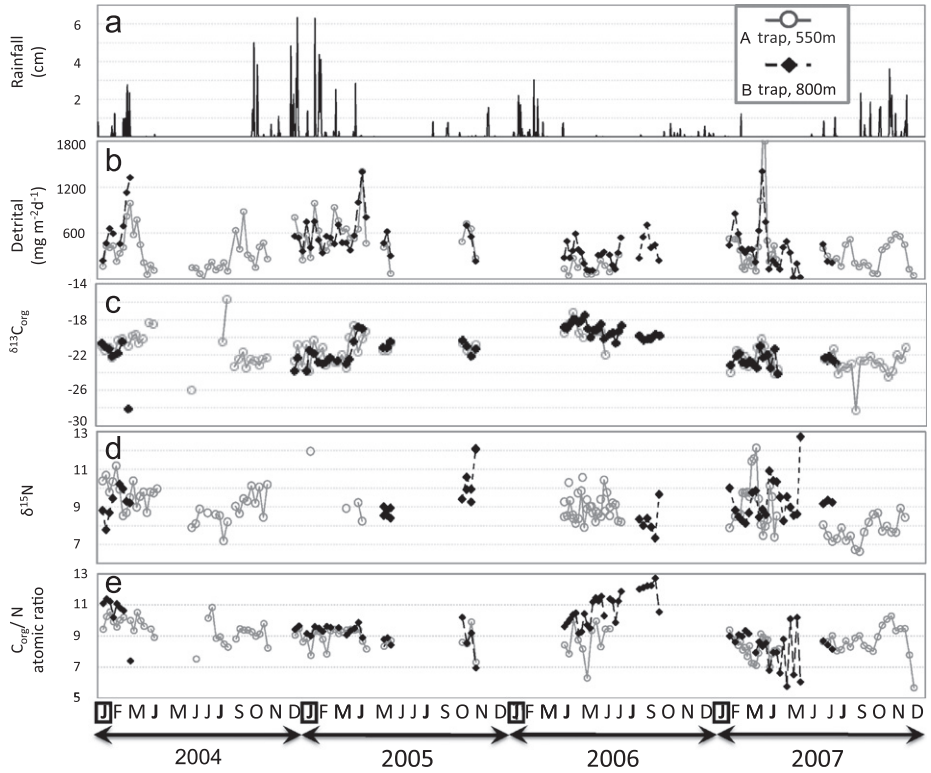

Fig. 4. (a) Rainfall (cm) at Long Beach Daugherty airfield; (b) flux of detrital (non-biogenic) material mg/m^2 d; (c) $\delta^{13}C_{org}$ values; (d) $\delta^{15}N$ values; (e) atomic C_{org}/N ratios.

Table 2
Monthly and annual average fluxes of mass, detrital, $bSiO_2$, total carbon, POC, PON, and $CaCO_3$. Monthly and annual average values of $\delta^{13}C$, $\delta^{13}C_{org}$, $\delta^{15}N$, and atomic C_{org}/N. Monthly averages were compiled using all 4 years of time series data for each month. Annual average is the average of these monthly values. Monthly standard deviation and for annual averages is standard deviation of the mean.

Month	Depth (m)	*n*	Mass (mg/m^{2}d)	Mass ±	Detrital (mg/m^{2}d)	Detrital ±	$bSiO_2$ (mmol/m^{2}d)	$bSiO_2$ ±	Total carbon (mmol/m^{2}d)	Total carbon ±	POC (mmol/m^{2}d)	POC ±	PON (mmol/m^{2}d)	PON ±	$CaCO_3$ (mmol/m^{2}d)	$CaCO_3$ ±	$\delta^{13}C$	$\delta^{13}C$ ±	$\delta^{13}C_{org}$	$\delta^{13}C_{org}$ ±	$\delta^{15}N$	$\delta^{15}N$ ±	Atomic C_{org}/N	Atomic C_{org}/N ±
Jan	550	10	580	83	374	53	1.35	0.54	3.30	0.52	2.70	0.46	0.29	0.05	0.60	0.08	−17.7	0.2	−21.8	0.4	9.9	0.4	9.4	0.2
Feb	550	16	547	76	333	46	1.41	0.27	3.14	0.39	2.53	0.34	0.28	0.04	0.61	0.06	−17.4	0.2	−22.1	0.3	9.6	0.2	8.8	0.2
Mar	550	19	790	155	489	100	2.23	0.58	5.12	0.91	4.20	0.75	0.47	0.08	0.93	0.16	−17.1	0.3	−21.2	0.3	9.3	0.3	8.9	0.2
Apr	550	13	752	251	351	126	3.05	1.07	5.89	1.49	5.06	1.25	0.55	0.14	1.03	0.25	−17.2	0.2	−20.7	0.5	9.4	0.2	8.4	0.3
May	550	6	453	102	176	54	1.44	0.38	4.66	0.99	4.00	0.94	0.46	0.09	0.67	0.13	−−17.9	0.3	−20.0	0.8	9.2	0.3	8.6	0.5
Jun	550	8	281	25	126	19	0.67	0.08	2.74	0.24	2.28	0.17	0.24	0.03	0.52	0.15	−16.4	1.2	−21.5	1.2	8.7	0.2	9.1	0.3
Jul	550	9	465	61	227	45	1.55	0.28	4.57	0.36	3.73	0.26	0.41	0.03	0.84	0.14	−16.9	0.4	−22.6	0.6	8.0	0.2	9.4	0.3
Aug	550	7	410	50	230	52	0.94	0.06	3.54	0.33	2.75	0.26	0.32	0.03	0.79	0.10	−17.3	0.6	−22.4	1.7	7.6	0.2	8.7	0.5
Sep	550	9	472	84	274	54	0.96	0.17	3.61	0.52	2.84	0.40	0.32	0.05	0.77	0.13	−17.9	0.3	−22.7	0.2	8.6	0.3	9.0	0.2
Oct	550	12	507	67	312	41	0.85	0.12	4.16	0.71	3.55	0.67	0.40	0.08	0.61	0.07	−18.5	0.2	−22.5	0.3	9.2	0.4	9.1	0.2
Nov	550	3	539	34	426	31	0.69	0.04	2.99	0.10	2.43	0.08	0.26	0.01	0.56	0.03	−19.1	0.1	−22.0	0.4	8.3	0.4	9.0	0.5
Dec	550	5	389	144	258	97	0.53	0.18	2.49	0.78	2.06	0.63	0.24	0.06	0.43	0.15	−18.5	0.1	−22.3	0.7	N/A	N/A	8.1	0.6
Annual average	*550*		*516*	*42*	*298*	*30*	*1.31*	*0.21*	*3.85*	*0.30*	*3.18*	*0.26*	*0.35*	*0.03*	*0.70*	*0.05*	*−17.7*	*0.2*	*−21.8*	*0.2*	*8.9*	*0.2*	*8.9*	*0.1*
Jan	800	10	651	116	428	59	1.49	0.67	3.55	0.78	2.88	0.64	0.30	0.08	0.67	0.15	−17.9	0.18	−22.1	0.3	8.9	0.2	9.9	0.3
Feb	800	14	700	108	456	59	1.67	0.32	3.95	0.70	3.08	0.53	0.33	0.06	1.03	0.29	−17.6	0.1	−22.9	0.5	9.1	0.2	9.6	0.3
Mar	800	11	755	159	458	100	2.42	0.66	4.96	1.03	4.12	0.83	0.47	0.10	0.85	0.21	−18.1	0.2	−22.0	0.5	9.2	0.3	8.7	0.3
Apr	800	14	953	145	457	73	4.25	0.67	6.73	0.93	5.82	0.79	0.66	0.10	0.90	0.30	−17.4	0.2	−19.4	0.6	9.2	0.2	8.9	0.4
May	800	12	447	94	198	39	1.90	0.53	4.07	0.89	3.73	0.88	0.39	0.09	0.41	0.10	−17.8	0.2	−19.5	0.4	9.0	0.4	9.6	0.5
Jun	800	7	370	60	200	26	1.00	0.25	3.35	0.63	2.91	0.51	0.31	0.07	0.30	0.11	−18.4	0.1	−19.9	0.3	9.3	0.2	10.6	0.4
Jul	800	5	597	75	336	48	2.02	0.23	4.95	0.56	4.25	0.62	0.43	0.04	0.70	0.23	−17.6	0.3	−21.0	0.8	8.8	0.3	9.7	0.8
Aug	800	3	524	121	358	89	0.79	0.15	3.33	0.72	3.03	0.68	0.25	0.05	0.29	0.05	−18.5	0.1	−20.1	0.1	8.3	0.1	12.3	0.1
Sept	800	3	378	65	259	44	0.62	0.11	2.49	0.41	2.36	0.38	0.20	0.02	0.13	0.03	−18.9	0.1	−20.0	0.2	8.3	0.7	11.8	0.7
Oct	800	4	689	157	354	84	0.84	0.20	5.75	1.40	5.19	1.27	0.58	0.11	0.57	0.15	−19.0	0.4	−21.2	0.4	10.5	0.6	8.7	0.7
Nov	800	0	N/A	N/A	N/A	N/A	N/A	N/A	N/A	N/A	N/A	N/A	N/A	N/A	N/A	N/A	N/A	N/A	N/A	N/A	N/A	N/A	N/A	N/A
Dec	800	3	514	67	341	44	0.70	0.09	3.41	0.19	2.74	0.15	0.29	0.02	0.67	0.04	−18.2	0.3	−23.1	0.7	N/A	N/A	9.5	0.1
Annual average	*800*		*598*	*53*	*350*	*29*	*1.61*	*0.32*	*4.23*	*0.38*	*3.65*	*0.33*	*0.38*	*0.04*	*0.59*	*0.09*	*−18.1*	*0.2*	*−21.0*	*0.4*	*9.1*	*0.2*	*9.9*	*0.4*

Table 3
Monthly and annual average fluxes of mass, detrital, $bSiO_2$, total carbon, POC, PON, and $CaCO_3$. Monthly and annual average values of $\delta^{13}C$, $\delta^{13}C_{org}$, $\delta^{15}N$, and atomic C_{org}/N. Data was used for calculations only when both traps successfully sampled or collected. Monthly averages were compiled using all 4 years of time series data for each month. Annual average is the average of these monthly values. Monthly standard deviation and for annual averages is standard deviation of the mean.

Month	Depth (m)	*n*	Mass (mg/m^{2}d)	Mass ±	Detrital (mg/m^{2}d)	Detrital ±	$bSiO_2$ (mmol/m^{2}d)	$bSiO_2$ ±	Total carbon (mmol/m^{2}d)	Total carbon ±	POC (mmol/m^{2}d)	POC ±	PON (mmol/m^{2}d)	PON ±	$CaCO_3$ (mmol/m^{2}d)	$CaCO_3$ ±	$\delta^{13}C$	$\delta^{13}C$ ±	$\delta^{13}C_{org}$	$\delta^{13}C_{org}$ ±	$\delta^{15}N$	$\delta^{15}N$ ±	Atomic C_{org}/N	Atomic C_{org}/N ±
Jan	550	9	580	88	374	56	1.35	0.57	3.30	0.55	2.71	0.48	0.29	0.06	0.60	0.09	−17.7	0.2	−21.8	0.4	9.9	0.5	9.4	0.3
Feb	550	14	585	82	352	50	1.52	0.29	3.36	0.42	2.71	0.36	0.32	0.04	0.65	0.06	−17.3	0.2	−22.0	0.3	9.4	0.2	9.0	0.2
Mar	550	14	874	200	556	128	2.58	0.75	5.24	1.17	4.36	0.97	0.50	0.11	0.90	0.20	−17.6	0.2	−21.5	0.4	9.2	0.4	8.6	0.2
Apr	550	10	863	157	403	119	3.55	0.47	6.68	0.43	5.86	0.51	0.66	0.08	1.23	0.08	−17.2	0.1	−21.2	0.3	9.2	0.2	8.3	0.4
May	550	6	453	125	176	66	1.44	0.46	4.66	1.22	4.10	1.23	0.46	0.11	0.67	0.16	−17.9	0.4	−20.0	0.9	9.2	0.4	8.6	0.7
Jun	550	5	253	33	112	22	0.69	0.12	2.57	0.28	2.32	0.27	0.25	0.03	0.31	0.04	−18.2	0.1	−20.3	0.6	8.9	0.2	9.4	0.3
Jul	550	4	613	32	322	38	2.29	0.07	5.12	0.39	4.15	0.38	0.46	0.03	0.98	0.09	−17.6	0.2	−22.1	0.3	7.8	0.3	8.9	0.2
Aug	550	0	N/A	N/A	N/A	N/A	N/A	N/A	N/A	N/A	N/A	N/A	N/A	N/A	N/A	N/A	N/A	N/A	N/A	N/A	N/A	N/A	N/A	N/A
Sep	550	0	N/A	N/A	N/A	N/A	N/A	N/A	N/A	N/A	N/A	N/A	N/A	N/A	N/A	N/A	N/A	N/A	N/A	N/A	N/A	N/A	N/A	N/A
Oct	550	4	689	115	389	69	1.08	0.23	6.44	1.48	5.80	1.35	0.68	0.16	0.63	0.16	−19.1	0.3	−21.2	0.2	10.2	0.6	8.6	0.5
Nov	550	0	N/A	N/A	N/A	N/A	N/A	N/A	N/A	N/A	N/A	N/A	N/A	N/A	N/A	N/A	N/A	N/A	N/A	N/A	N/A	N/A	N/A	N/A
Dec	550	3	574	161	379	112	0.78	0.19	3.48	0.89	2.85	0.73	0.31	0.08	0.63	0.16	−18.5	0.1	−22.3	0.7	N/A	N/A	8.9	0.2
Annual average	*550*		*609*	*64*	*340*	*43*	*1.70*	*0.31*	*4.54*	*0.49*	*3.87*	*0.44*	*0.44*	*0.05*	*0.73*	*0.09*	*−17.9*	*0.2*	*−21.4*	*0.3*	*9.2*	*0.3*	*8.9*	*0.1*
Jan	800	10	651	116	428	59	1.49	0.67	3.55	0.78	2.88	0.64	0.30	0.08	0.67	0.15	−17.9	0.2	−22.1	0.3	8.9	0.2	9.9	0.3
Feb	800	14	700	108	456	59	1.67	0.32	3.95	0.70	3.09	0.53	0.33	0.06	1.03	0.29	−17.6	0.1	−22.9	0.5	9.1	0.2	9.6	0.3
Mar	800	11	755	159	458	100	2.42	0.66	4.96	1.03	4.12	0.84	0.45	0.10	0.85	0.21	−18.1	0.2	−22.0	0.4	9.2	0.3	8.7	0.3
Apr	800	11	950	175	439	84	4.26	0.82	6.49	1.07	5.89	1.00	0.65	0.10	0.64	0.14	−17.3	0.2	−19.5	0.6	9.2	0.3	9.2	0.4
May	800	7	461	116	215	61	1.74	0.45	4.10	1.07	3.72	0.97	0.37	0.10	0.47	0.15	−17.9	0.3	−19.6	0.5	8.6	0.2	10.2	0.4
Jun	800	7	370	60	200	26	1.00	0.25	3.35	0.63	2.95	0.52	0.31	0.07	0.30	0.11	−18.4	0.1	−19.9	0.3	9.3	0.2	10.6	0.4
Jul	800	4	557	83	317	57	1.94	0.27	4.57	0.54	3.74	0.46	0.41	0.04	0.83	0.24	−17.5	0.3	−21.6	0.8	9.0	0.3	9.1	0.7
Aug	800	0	N/A	N/A	N/A	N/A	N/A	N/A	N/A	N/A	N/A	N/A	N/A	N/A	N/A	N/A	N/A	N/A	N/A	N/A	N/A	N/A	N/A	N/A
Sept	800	0	N/A	N/A	N/A	N/A	N/A	N/A	N/A	N/A	N/A	N/A	N/A	N/A	N/A	N/A	N/A	N/A	N/A	N/A	N/A	N/A	N/A	N/A
Oct	800	4	689	157	354	84	0.84	0.20	5.75	1.40	5.19	1.27	0.58	0.11	0.57	0.15	−19.0	0.4	−21.2	0.4	10.5	0.6	8.7	0.7
Nov	800	0	N/A	N/A	N/A	N/A	N/A	N/A	N/A	N/A	N/A	N/A	N/A	N/A	N/A	N/A	N/A	N/A	N/A	N/A	N/A	N/A	N/A	N/A
Dec	800	3	514	67	341	44	0.70	0.09	3.41	0.19	2.74	0.15	0.26	0.03	0.67	0.04	−18.2	0.3	−23.1	0.6	N/A	N/A	9.5	0.1
Annual average	*800*		*628*	*58*	*357*	*33*	*1.78*	*0.36*	*4.46*	*0.37*	*3.82*	*0.37*	*0.41*	*0.04*	*0.67*	*0.07*	*−18.0*	*0.2*	*−21.3*	*0.5*	*0.1*	*0.2*	*9.5*	*0.2*

magnitude of the fluxes caught in the two traps are nearly identical. The largest fluxes of mass, POC, N, $CaCO_3$ and $bSiO_2$ occur between February and June, and the length of the high flux period can be as short as 7 days or as long as 30 days. Of the biogenic constituents, only $CaCO_3$ has some tendency to show high or low flux patterns independent of the other constituents.

The annual average of all fluxes were determined by averaging monthly mean fluxes to account for over and under sampling distribution; thus 12 monthly averages were obtained from each depth. The annual average mass flux into the A and B traps was 516 ± 42 and 598 ± 53 mg/m^2 d, respectively. However, the two traps were operational over slightly different time intervals, and thus the annual average mass flux for the B trap is biased by fewer data in general and in particular from July to December when mass fluxes in the SPB are typically low. The range in mass flux is highly variable, from 81 to 2730 mg/m^2 d (Table 1), with highest fluxes in March–April. Although the timing and magnitude of the high springtime mass flux is variable from year to year, it coincides with the maximum flux of POC (Tables 2 and 3).

The coherence of the timing and magnitude of the fluxes captured in the A and B traps was excellent (Figs. 3 and 4). During deployment 8 (January–May 2007), the A trap cups were programmed to remain open for 4 days and the B trap cups for 6 days. For flux patterns to be identical in traps that were 250 m apart, a similar amount of particles must be falling for at least half the time that both cups are open during the same time period. Based on the timing and the distance between the two traps, particle settling velocities are constrained as 83–125 m/d (i.e. 250 m/3 days, 250 m/2 days) or faster.

4.1.1. Particulate organic carbon and nitrogen mass fluxes

The average annual POC flux into the trap at 550 m was 3.18 ± 0.26 mmol/m^2 d. POC fluxes were highest in the spring, but the timing of the high flux period differed each year, and some years captured multiple high flux events (i.e. 2007). March, April, and May were consistently high POC flux months. The POC flux correlates well with mass and $bSiO_2$ fluxes ($r=0.89$, $p=0.0001$ and $r=0.90$, $p=0.0001$, respectively); although, during low flux periods, the POC flux showed greater variability than the $bSiO_2$ flux (Fig. 3). The average annual PON flux into the trap at 550 m was 0.35 ± 0.03 mmol/m^2 d. The temporal distribution of high and low fluxes of PON fluxes was similar to that of POC.

C_{org}/N molar ratios varied between 7 and 11 and also show no clear pattern associated with the time of year or high POC flux events (Fig. 4). Annual average C_{org}/N ratios were 8.9 ± 0.1 (standard deviation) and 9.9 ± 0.4 at the 550 and 800 m traps, respectively, although uncertainty in wt% C_{org} and wt% N measurements further increases the uncertainty of this ratio to approximately ± 1.5 for both traps. The C_{org}/N ratios of the floating traps varied considerably, but the average was 9.7, similar to the deep traps.

4.1.2. $\delta^{13}C$ and $\delta^{15}N$ of organic matter

Most $\delta^{13}C_{org}$ values ranged between -18‰ and -24‰, although there are occasionally values as light as -28‰ and as heavy as -15‰ (Fig. 4). Both A and B traps record similar isotopic values and have similar annual average $\delta^{13}C_{org}$ of -21.8 ± 0.2‰ and -21.0 ± 0.4‰ (± 1 standard deviation of the mean) at 550 and 800 m, respectively. The average values we obtained are almost identical to values reported by Thunell et al. (1994b) from a trap at 500 m in SPB (average $\delta^{13}C_{org}$ of -22.1 ± 0.6‰, sample standard deviation). Sediment trap $\delta^{15}N$ values ranged from 7‰ to 11‰ with an average annual value at 550 m of 8.9 ± 0.2‰ and 9.1 ± 0.2‰ at 800 m, similar to the $\delta^{15}N$ of NO_3^- in the SPB water column, ~8‰ to 11‰ (Liu and Kaplan, 1989).

4.1.3. Bacterial abundance

Particle-associated bacteria were enumerated for sediment trap samples collected between January 2004 and September 2006. The average flux of bacteria to 550 and 800 m was $2.4 \pm 0.2 \times 10^{10}$ and $1.8 \pm 0.3 \times 10^{10}$ cells/m^2 d, respectively (± 1 standard error of the mean, where $n_{550}=83$ and $n_{800}=63$). The number of bacteria per mg of dry sediment averaged $5.9 \pm 0.6 \times 10^7$ and $2.7 \pm 0.3 \times 10^7$ at 550 and 800 m, respectively. For this 2-year period, the flux of bacteria was most closely correlated with the flux of $CaCO_3$ ($r=0.63$, $p=0.0001$) followed by fluxes for mass ($r=0.44$, $p=0.0001$), detrital material ($r=0.34$, $p=0.0001$), $bSiO_2$ ($r=0.32$, $p=0.0002$), PON ($r=0.3$, $p=0.0006$) and POC ($r=0.28$, $p=0.001$).

4.1.4. Inorganic carbon fluxes

Fluxes of $CaCO_3$ most closely correspond to variations in the mass and POC fluxes. However, there are a few large mass and POC pulses that do not have large associated fluxes of $CaCO_3$ (e.g. April 2006, Fig. 3). The average annual $CaCO_3$ flux to the A trap was 0.70 ± 0.05 mmol/m^2 d and to the B trap it was 0.59 ± 0.09 mmol/m^2 d. In general, 2006 was a low $CaCO_3$ flux year.

4.1.5. Biogenic silica fluxes

The largest fluxes of $bSiO_2$ coincide with the largest mass and POC fluxes, which occur in the springtime. The average annual flux to 550 m was 1.31 ± 0.21 mmol/m^2 d. $bSiO_2$ fluxes tend to be low (<1 mmol/m^2 d) for most of the year, and then very high (>4 mmol/m^2 d) during spring blooms (Fig. 3).

4.1.6. Detrital fluxes

Detrital fluxes varied from 12 to 1200 mg/m^2 d and contribute 5–75% of the total mass flux, with an average of 50% of the total mass of settling particles. The annual average detrital flux at 550 m was 298 ± 30 mg/m^2 d.

4.2. Short-term floating trap fluxes tethered at 100 and 200 m

Fluxes of mass, total carbon, POC, PON, $CaCO_3$, and $bSiO_2$ were determined from floating traps suspended at 100 and 200 m (Table 4). Generally, the mass, POC, PON, and $CaCO_3$ fluxes obtained from these trap deployments were greater than those values from the deep traps, although they represent only a 24 h snapshot of flux, and there is considerable literature regarding the accuracy of floating trap data (Buesseler, 1991; Buesseler et al., 2007a; Gardner, 1980; Honjo et al., 2008) and references therein. On average, the floating traps captured a lower flux of detrital matter and $bSiO_2$ than the deep traps.

The average mass flux captured at 100 and 200 m was 650 ± 240 and 640 ± 280 mg/m^2 d, respectively (± 1 standard deviation). The floating traps captured 1.4 ± 0.6 and 1.3 ± 0.6 mmol/m^2 d $bSiO_2$ at 100 and 200 m. The average POC fluxes caught by the floating traps were 11.2 ± 5.1 mmol/m^2 d at 100 m and 9.1 ± 4.4 mmol/m^2 d at 200 m. The detrital flux averaged 169 ± 121 mg/m^2 d at 100 m and 151 ± 69 mg/m^2 d at 200 m. The average N fluxes were 1.4 ± 1.0 mmol/m^2 d at 100 m and 1.3 ± 0.7 mmol/m^2 d at 200 m.

4.3. Climatology

Because of its Mediterranean climate, rainfall years for this region run from October to September. The 4-year period that the traps were deployed captured one of the wettest (2004–2005; 74.6 cm) and one of the driest (2006–2007; 6.6 cm) years on record in Southern California. It has been demonstrated that

Table 4
Floating sediment trap data from 100 and 200 m. Detrital fluxes calculated as in text, uncertainty ±30% of value reported. Average uncertainty of $bSiO_2$ ±10% of reported values. Wt% PON ±1% of reported values. Total carbon (TC) ±6.5% of reported values. Wt% C_{org} ±10% of reported values.

DATE	Duration (hrs) in water	Depth (m)	Mass (mg)	Mass stdev	Mass flux (mg/m^2d)	$bSiO_2$ ($mmol/m^2d$)	$CaCO_3$ flux ($mmol/m^2d$)	POC flux ($mmol/m^2d$)	PON Flux ($mmol/m^2d$)	Detrital flux (mg/m^2d)	wt% $bSiO_2$	wt% PON	wt% TC	wt% C_{org}	wt% TIC	Atomic C_{org}/N
5.19.05	48	100	N/A	N/A	1446	3.7	8.0	28.1	5.2	0	15.5	5.1	30.0	23.3	6.7	5.4
5.19.05	48	200	N/A	N/A	1573	3.0	6.0	23.9	3.6	353	11.3	3.2	22.8	18.2	4.6	6.7
11.15.07	4.3	100	1.06	0.9	782	1.3	10.8	4.0	1.1	451	9.9	1.9	22.8	6.1	16.7	3.7
11.15.07	3.5	100	2.10	1.0	1834	2.0	8.3	12.4	0.8	1143	6.7	0.6	13.6	8.1	5.5	15.5
11.28.07	4.5	100	0.40	0.3	246	0.1	3.8	3.3	0.4	121	3.1	2.2	34.8	16.1	18.7	8.6
12.11.07	24.4	100	1.31	0.5	162	0.1	N/A	N/A	0.13	N/A	4.1	1.1	14.2	N/A	N/A	N/A
4.3.08	19.5	100	2.71	0.7	335	0.7	0.2	4.8	0.5	84	11.9	1.9	17.7	17.1	0.6	10.2
4.3.08	19.5	200	3.58	0.8	443	1.2	0.3	7.6	1.0	22	16.0	3.2	21.4	20.5	0.9	7.6
4.16.08	17.2	100	1.50	0.2	185	0.05	0.6	2.5	0.2	101	1.6	1.3	20.0	16.1	3.9	14.2
4.16.08	17.4	200	2.03	0.2	251	0.1	0.9	3.6	0.4	120	2.8	2.1	21.3	17.1	4.3	9.3
5.7.08	17.1	100	3.61	0.4	445	1.5	1.2	6.4	0.6	13	20.6	2.0	20.6	17.3	3.2	10.2
5.7.08	17.1	200	2.68	0.7	331	1.3	1.1	4.5	0.5	0	22.9	2.0	20.3	16.3	4.0	9.4
6.18.08	25	200	2.36	0.4	291	0.2	0.5	2.5	0.4	182	3.6	2.1	12.6	10.5	2.2	5.8
Average	–	100	–	–	650 ± 240	1.4 ± 0.6	4.7 ± 4.3	11.2 ± 5.1	1.4 ± 1.0	169 ± 121	–	–	–	–	–	–
Average	–	200	–	–	640 ± 280	1.3 ± 0.6	1.8 ± 2.4	9.1 ± 4.4	1.3 ± 0.7	151 ± 69	–	–	–	–	–	–

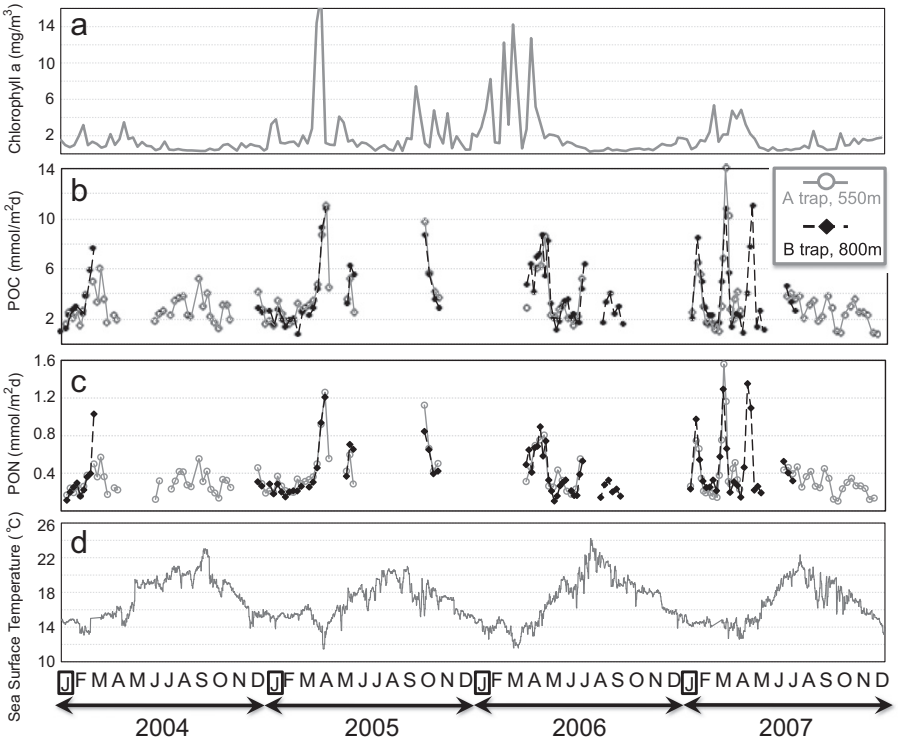

Fig. 5. (a) San Pedro Ocean Time series (SPOTs) chlorophyll *a* (mg/m^3) from SeaWiFS satellite (27 km × 27 km); (b) particulate organic carbon flux ($mmol/m^2$ d), (c) particulate nitrogen flux ($mmol/m^2$ d); (d) sea surface temperature (°C) from NOAA buoy 46222. This record covers 1/1/04 to 12/31/07.

regional rainfall and runoff are temporally well correlated (Gorsline, 1978; Thunell et al., 1994b). Rainfall events can last for a few hours or a few days, but rarely does it rain for longer than a few consecutive days in Southern California. Thus the spiky trend in rainfall demarcates rainfall events (Fig. 4).

Sea surface temperatures (SST) show seasonal variation (Fig. 5) with the warmest surface water observed in late July through September (average = 20.0 °C). The coolest surface waters typically occur from February to early May (average = 14.3 °C), although a cold SST anomaly is sometimes detected at other times of the year. The average summer SST in 2006 was >1 °C warmer and occurred earlier (July) than the other years sampled.

Satellite chlorophyll data was examined for a 27 km × 27 km area centered on the SPOT site. Both POC and $bSiO_2$ fluxes showed significant correlations with satellite-derived estimates of chlorophyll *a*; the Pearson correlation coefficients are weak but statistically significant ($r_{POC}=0.25$, $p=0.0014$; $r_{bSiO_2}=0.28$, $p=0.0002$).

5. Discussion

Previous work in the SPB (Thunell et al., 1994b) attributed biogenic fluxes to springtime upwelling and lithogenic fluxes to rainfall events. Their study found that following rainfall, the C_{org}/N ratios of particles increased, and the $\delta^{13}C_{org}$ got lighter, which was interpreted to indicate a higher contribution of terrestrial organic carbon input to POC fluxes in SPB. Thunell

et al. (1994b) found this pattern was most prominent in January and February, and associated with two rainfall events. Thunell et al. (1994b) also found that spring upwelling (April–June) was associated with higher fluxes of organic matter, biogenic silica, and $CaCO_3$. Thunell and colleagues also documented the ecological progression of carbonate-forming organisms as represented in sediment trap foraminifera and coccolithophores (Sautter and Thunell, 1991; Ziveri et al., 1994). Our time series of sediment traps showed many similar, yet some different, results from Thunell et al. (1994b), in part because of the length of our study was sufficient to account for seasonal and inter-annual variability over 4 years. A compilation of all long-term (> 20 days) sediment trap work in SPB and the adjoining Santa Monica Basin is presented in Table 5.

5.1. Timing and sources of detrital sedimentation

We examined the timing and magnitude of rainfall events relative to trap fluxes of detrital material, C_{org}/N ratios, $\delta^{13}C_{org}$ and $\delta^{15}N$ of the organic matter to help constrain the importance of runoff to particle export. We generally see a poor correlation between integrated rainfall and tracers of continentally derived sedimentation ($r_{C/N}=-0.04$, $p=0.61$; $r_{\delta^{13}C_{org}}=-0.12$, $p=0.06$; $r_{\delta^{15}N}=0.20$, $p=0.01$) (Fig. 5). The average detrital flux from January through May versus total rainfall (cm) from October through May shows modest, but not significant correlation ($r=0.59$, $p=0.42$). Moreover, both 2003–2004 and 2005–2006 had similar rainfall amount (18.2 and 21.0 cm, respectively), yet their average detrital fluxes vary by a factor of 2 (338 ± 44 and 154 ± 21 mg/m^2 d). The highest (74.5 cm) and lowest (6.6 cm) rainfall years (2004–2005 and 2006–2007, respectively) were more similar in their magnitude of detrital fluxes (414 ± 38 and 303 ± 43 mg/m^2 d) than 2003–2004 and 2005–2006, when rainfall quantity was almost identical. The continuity of trap operation through the wettest periods (January–April) was good for all these intervals, thus the record of trap flux and rainfall events is quite robust. It is possible to find some correspondence in rain followed by a pulse of detrital flux on an event-by-event basis (e.g. February–March 2004), yet the 4-year time record shows this is not necessarily observed every year. Over multiple rainy seasons, rainfall and detrital sedimentation are poorly correlated.

The $\delta^{13}C$ of organic matter collected in the moored traps indicates that large rainfall events generally do not contribute a significant amount of terrestrial organic carbon to the sediment traps since the $\delta^{13}C$ of the organic carbon collected in the traps (-21.8 ± 0.2‰ and -21.0 ± 0.4‰ at 550 and 800 m, respectively), is similar to the average $\delta^{13}C$ of marine phytoplankton (-18‰ to -22‰; Degens, 1969). While a few rainfall events correspond to isotopically light excursions of $\delta^{13}C_{org}$, which is expected if runoff is carrying isotopically lighter terrestrially derived POC (as observed by Thunell et al., 1994b), these data are not representative of the 4-year trend; we observe little correlation between isotopic excursion of $\delta^{13}C_{org}$ and rainfall amount ($r=-0.12$, $p=0.10$; see Fig. 4).

Trap material C_{org}/N ratios are considerably higher than the canonical Redfield value of 6.7 ($C_{org}/N_{avgsurf.}=9.7$; $C_{org}/N_{avg550}=8.9\pm0.1$; $C_{org}/N_{avg800}=9.9\pm0.4$) and can be as high as 11.5, which could indicate some POC input from non-marine sources (Perdue and Koprivnjak, 2007). However, fluctuations in C_{org}/N do not correlate with the timing or magnitude of rainfall (Fig. 4). The expected trend for $\delta^{15}N$ isotopes, if a component of the organic matter were terrestrially derived, would be high C_{org}/N correlating with light $\delta^{15}N$ values; Fig. 6 shows no significant correlation between C_{org}/N and $\delta^{15}N$ for particles collected at 550 m; particles collected at 800 m have a significant negative correlation, which could be consistent with some terrigenous input ($r_{550}=-0.20$, $p=0.06$; $r_{800}=-0.57$, $p=0.0001$). Previous sediment trap work in SPB by Nelson et al. (1987) found average C_{org}/N values of 9.3 ± 0.6 ($n=3$) at 500 m and average values from 100 to 824 m of 8.8 ± 1.0 ($n=8$). Additionally, Thunell

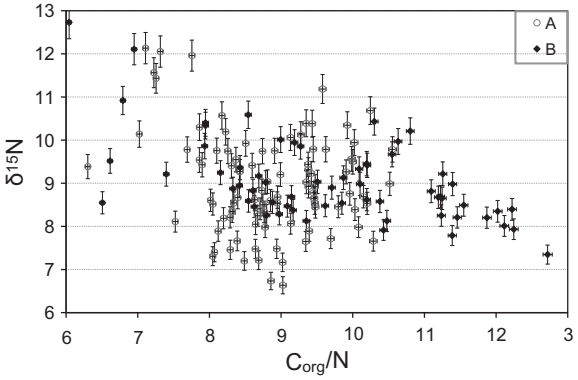

Fig. 6. $\delta^{15}N$ versus atomic C_{org}/N.

Table 5
Summary of average sediment fluxes reported for San Pedro and Santa Monica Basins references are a) Crisp et al. (1979); b) Bruland et al. (1981); c) Nelson et al. (1987); d) Thunell et al. (1994a, 1994b); e) Huh et al. (1993); ∗ this study.

Reference	Location	Date of trap deployment	Depth (m)	# of days trapping	Average mass flux (mg/m^2 d)	Average POC flux (mmol/m^2 d)	Average $CaCO_3$ flux (mmol/m^2 d)	Average atomic C_{org}/N	Average $bSiO_2$ flux (mmol/m^2 d)
a	SPB	1977	879	55	767	2.9	–	–	–
a	SMB	1977	892	55	493	2.5	–	–	–
b	SPB	1977	870	55	997	–	–	–	–
b	SMB	1977	870	55	463	–	–	–	–
c	SPB	1983	500	190	270	1.3	0.6	9.3	–
c	SPB	1983	824	190	421	2.0	0.9	10.1	–
d	SMB	1986–1990	50	197	761	20.0	–	–	–
d	SMB	1986–1990	100	451	487	10.4	–	–	–
d	SMB	1986–1990	150	806	621	10.1	–	–	–
d	SMB	1986–1990	200	209	491	7.1	–	–	–
d	SMB	1986–1990	300	197	609	7.0	–	–	–
d	SMB	1986–1990	500	863	518	4.3	–	–	–
d	SMB	1986–1990	700	863	591	4.1	–	–	–
d	SMB	1986–1990	850	983	588	3.9	–	–	–
e	SPB	1988	500	182	514	2.7	0.9	8.7	1.16
*	SPB	2004–2008	550	793	516	3.2	0.7	8.8	1.31
*	SPB	2004–2008	800	536	598	3.6	0.6	9.9	1.61

et al. (1994b) found average C_{org}/N ratios at 500 m of 8.7 ± 1.6 ($n=26$). Both of these studies along with ours suggest the C_{org}/N ratio in San Pedro Basin is higher than the canonical Redfield ratio, remains high during the non-rainy portion of a year and cannot be explicitly related to terrestrial inputs.

It is acknowledged here that the tracers applied to characterize terrestrially derived C_{org} are not highly specific. High C_{org}/N ratios can be acquired by preferential loss of N in sinking particles, and the $\delta^{15}N$ of the sinking flux is influenced by fractionation associated with nitrate assimilation in SPB surface waters, where surface nitrate concentrations can rise to 1–2 μM during the winter months. The presence of unconsumed nitrate in surface waters in SPB would generate a sinking flux with a lower $\delta^{15}N$ during the beginning of periods of high productivity, and the $\delta^{15}N$ of the sinking flux would slowly rise as nitrate is drawn down during the late spring and early summer, consistent with the range in $\delta^{15}N$ observed in some trap samples. Additionally, atmospheric deposition has been shown to have a low-$\delta^{15}N$ (Hastings et al., 2003; Knapp et al., 2010) and nitrogen fixation could also contribute to low $\delta^{15}N$ of the sinking flux, especially during the summer and fall when biological productivity is lower compared to the winter and spring. Low $\delta^{13}C_{org}$ values may also be acquired in a variety of ways, although the simplest interpretation is that $\delta^{13}C_{org} < -24‰$ indicates the introduction of some terrestrially sourced C_{org}.

We see no evidence from isotope data that rain events consistently contribute to terrestrially derived C_{org} flux to the SPOT site, 15 km offshore. Rainfall events, especially the large storms, generate runoff from the LA River, the San Gabriel River, and the Santa Ana River; this creates plumes of discolored water recognizable from satellite images, and they can extend up to 15 km offshore (Nezlin and DiGiacomo, 2005; Nezlin et al., 2005). Such plumes have also been noted in studies of runoff from the Santa Clara River, further to the north (Warrick et al., 2004). Yet plumes in the San Pedro Basin region typically propagate a few km offshore and then to the southeast, and do not extend into the area of SPB where our trap was located. While the runoff plumes from rivers adjacent to SPB do not appear to contribute to detrital fluxes, it is possible that river plumes from further north along the coastline could contribute to sediment fluxes. It is also possible that the sediment load associated with these plumes is deposited on the shelf and this detrital matter is slowly mobilized and distributed to the deeper ocean after some significant time lag.

Mass fluxes at 800 m range from 100 to 2130 mg/m^2 d with an annual average of 598 ± 53 mg/m^2 d. This flux is slightly lower than previous estimates of sediment accumulation rates for San Pedro Basin, which range from 822 to 2685 mg/m^2 d (Bruland et al., 1981; Emery, 1960; Nardin, 1981; Schwalbach, 1982; Schwalbach and Gorsline, 1985). However, these previous estimates are derived primarily by age dating of sediment cores or by seismic techniques. Such a geological assay of sediment accumulation will average sedimentation over tens of years or longer. As described below, the mass flux obtained by our traps is consistent with other trap flux data (Table 5) and with the current accumulation rate defined by ^{210}Pb in SPB sediments.

The magnitude of the POC flux is higher, and the detrital flux is lower in the floating traps deployed at 100 and 200 m compared to the fluxes of POC and detrital material caught in the 550 and 800 m traps (Tables 3 and 4). This suggests an increase in the average detrital flux between shallow traps and the 550 m moored trap, which, if the shallow floating trap data are representative, indicates that the major source of detrital material is not from the surface ocean. An alternative source of the detrital material to the deep traps would be the resuspension of shelf and slope sediments; particles from this environment may enter central basin waters as nepheloid layers (Drake and Gorsline, 1973) from which sinking and scavenging occurs. However, we show below that the increase in detrital flux with depth is not due to inputs of resuspended sediments from the basin floor directly surrounding the deep-moored traps. Finally, the floating sediment trap data also indicate that biogenic ballast ($CaCO_3$ and $bSiO_2$) is sufficient to export POC in the absence of much lithogenic ballast.

5.2. Sources and timing of biogenic fluxes

The strong correlation between POC and $bSiO_2$ ($r=0.90$, $p=0.0001$) suggests that in SPB a majority of the POC that sinks is associated with this biogenic mineral. This is supported by a qualitative examination of the trap material, where we find numerous diatoms in the high POC flux intervals.

Fig. 5 shows that the highest POC fluxes typically occur in the spring and are preceded by relatively cold SSTs. Maxima in surface ocean chlorophyll are generally synoptic throughout the Southern California Bight, but images of the region around the SPOT site show a weak but statistically significant correlation between chlorophyll *a* in surface waters and trap $bSiO_2$ flux (Collins, 2009). Buoy measurements of SST provide a reasonable predictor of upwelling, but SST will also be influenced by horizontal advection of different water masses. In some years, cold spikes in SST, likely due to intense upwelling, occur 1–2 weeks before a large POC flux event (Fig. 5). In other years, cold SSTs can occur either several days before or even after a large POC flux event. As with ocean color, SST is a good but imperfect predictor of the timing and magnitude of the POC flux. Conditions that may be specific to the SPOT location, such as the generation of eddies from interactions of the California Current with Catalina Island, may be one reason for the imperfect correlation between SST, surface ocean chlorophyll *a* and POC flux. The lack of a strong correlation between chlorophyll *a* and POC ($r=0.25$, $p=0.001$) probably also reflects the sensitivity of remote sensing of the upper few centimeters of the ocean, while the sediment trap flux reflects the integrated flux from the entire euphotic zone.

In consideration of the sources of POC to the traps, and its fate during settling, measurements were made of bacterial numbers and their contribution to POC fluxes. Average bacterial flux values of $2.4 \pm 0.2 \times 10^{10}$ and $1.8 \pm 0.3 \times 10^{10}$ cells/m^2 d at 550 and 800 m, respectively suggest that the bacterial flux may decline with depth, but this decline is not significant. This fluxes we found are similar to those at other sites (3.2×10^{10} cells/m^2 d in the NE Atlantic, Turley and Mackie, 1995; 2.6×10^9 cells/m^2 d in the Porcupine Abyssal Plain, Vanucci et al., 2001). Although bacterial fluxes at SPOT are poorly correlated with all flux constituents, they show the best correlation ($r=0.63$, $p=0.0001$) to the flux of $CaCO_3$.

Establishing the contribution of bacterial carbon to the C_{org} flux requires knowledge of bacterial carbon content, yet the range of published values for bacteria cellular C content varies by an order of magnitude (Fukuda et al., 1998; Vrede et al., 2002). The bacterial C_{org} content per cell that we use for calculations is based on the value for coastal marine bacteria (Fukada et al., 1998). Assuming each cell contains 30×10^{-15} g carbon, SPB trap material-associated bacteria account for <1–9% (an average of 1.7 ± 1.6%) of the POC flux. However, because of the large variation in C_{org} in bacterial cells and because we counted cells but did not measure cell size, it is possible that bacteria in our traps account for a larger fraction of C_{org} than we calculate. Further, work by Turley and Hughes (1992) has shown that after only 40 days of storage, the number of DAPI-countable bacterial cells fixed in formalin decrease up to 40%. Due to our sediment trap deployment length, we could not avoid storage (sometimes up to 6 months *in situ*) and so it is possible our bacterial counts are underestimated. Despite these complications, it seems unlikely that we have underestimated bacterial counts and cellular carbon content by as much as a factor

of 2. Taking this into account, the bacterial mass would still only account for $<8\%$ of the total POC flux.

5.3. Comparing the flux at 550 m versus 800 m

There is good coherence in the timing and magnitude of fluxes between traps: POC ($r_{550-800}=0.87$, $p=0.0001$), PON ($r_{550-800}=0.86$, $p=0.0001$), $bSiO_2$($r_{550-800}=0.87$, $p=0.0001$), and $CaCO_3$ fluxes ($r_{550-800}=0.52$, $p=0.0001$) (Figs. 3, 4, and 5). Small increases and decreases in the magnitudes of these fluxes are synchronous. The significant correlation between detrital and POC fluxes ($r=0.66$, $p=0.0001$) may indicate that detrital particles play a role in the ballasting of POC (Fig. 3; March 2004; April 2005). However, there are also periods where POC fluxes are high and detrital fluxes are not (Fig. 3; April 2006; February, May, and November 2007) which indicates that during certain periods, detrital material does not play the primary role in POC export.

To consider whether the samples in either Trap A or B contained significant material derived from sediment resuspension, we examined the wt% POC, $bSiO_2$, and $CaCO_3$ with cross plots (Fig. 7). Monthly differences in fluxes were compared for the two traps when both traps captured material (Table 3). There was no difference in flux between the two depths within the precision of measurement for $bSiO_2$, POC, and PON. Both average mass and detrital fluxes are larger at 800 m in June. $CaCO_3$ fluxes are larger at 800 m in February and larger at 500 m in April. The POC versus $bSiO_2$ plot shows both the A trap and B trap data are thoroughly intermixed, and so there is no indication that the deeper trap contains lower wt% POC or $bSiO_2$ compared to the shallower trap. This argues against a significant component derived from sediment resuspension as SPB sediments have much lower wt% C_{org} (3.34 ± 0.06, L. Collins, unpublished) and $bSiO_2$ (2.05 ± 0.51; Cheng et al., 2009) than the values observed in the B trap. If sediment resuspension were occurring, it would decrease the wt% POC and $bSiO_2$ in the B trap, which is not observed. The wt% $CaCO_3$ versus wt% POC cross plot also does not show the B trap skewed toward seafloor sediment composition. However, there are instances where lower fluxes of $CaCO_3$ are recorded in the B trap, or $CaCO_3$ makes up a lower fraction of the mass flux in the B trap.

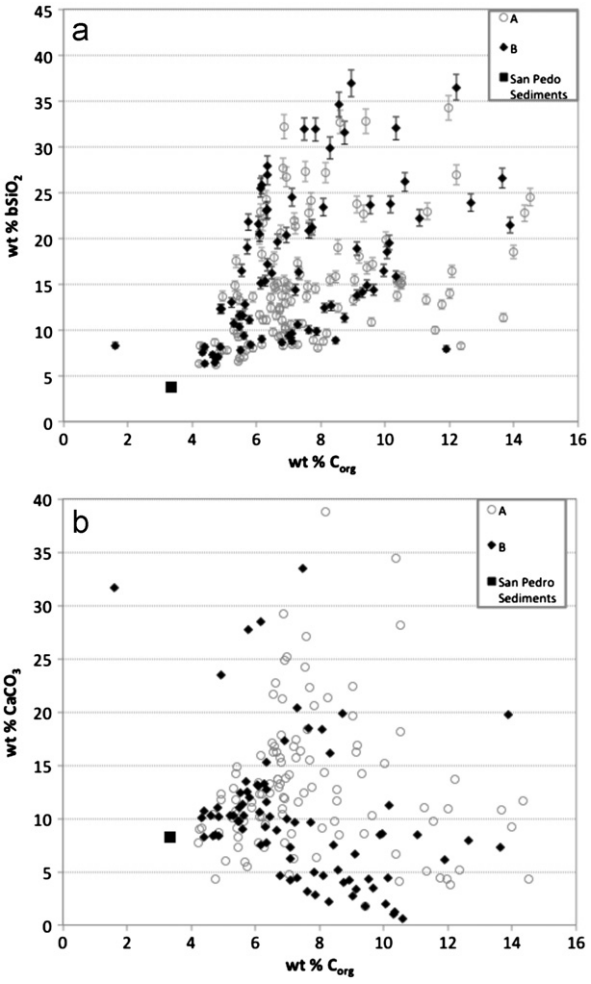

Fig. 7. (a) Wt% biogenic silica versus wt% C_{org}; (b) wt% $CaCO_3$ versus wt% C_{org} error bars for $CaCO_3$ are 0.06% and for C_{org} are 0.06% based on run of an internal standard of San Pedro Basin mud.

The significant correlation between mass fluxes captured in the 550 and 800 m traps suggest that issues such as variable trap efficiencies, inputs from lateral sources, and productivity occurring between trap depths did not cause significant differences in fluxes measured by the A and B traps. Surprisingly, these traps support the simplistic model that particle fluxes are derived from the surface ocean and that essentially, particles fall vertically at this site. The overall accuracy of the trap flux values was checked by making measurements of ^{210}Pb flux into the traps and calculating the ^{210}Pb inventory from a San Pedro Basin sediment core. Measured ^{210}Pb fluxes (dpm/cm^2 year) were 2.92 ± 0.25 in the 550 m trap, 3.23 ± 0.19 in the 800 m trap, and 3.05 ± 0.37 in the SPB sediment core. Although the 800 m trap captures a slightly larger (10%) ^{210}Pb flux than the 550 m trap, the uncertainty in each flux is also $\sim$10%. The mean trap flux value is within 5% of the sediment inventory of excess ^{210}Pb measured in the 2006 core (Fig. 2), and is also consistent with the ^{210}Pb profiles in cores analyzed by Huh et al. (1990). Water column production of ^{210}Pb could only support about 15%, and atmospheric input $<5\%$ (Fuller and Hammond, 1983) of the observed flux. Similarly, Bruland et al. (1974) showed that most ^{210}Pb carried to these sediments must be brought in by lateral transport and scavenged by settling particles. If particle flux is generally vertical, the implication of these data is that currents are moving waters with high ^{210}Pb content into the path of settling particles. Alternatively, particles containing excess ^{210}Pb could be focused into this area, but the data indicate that any focusing must occur at depths shallower than 550 m. A model that accounts for nepheloid layer transport of detrital and ^{210}Pb-enriched materials could explain these data.

5.4. Floating and deep trap POC fluxes: the vertical distribution of fluxes

Comparisons of monthly average POC fluxes when both traps captured material show that there is no difference between the magnitude of the POC fluxes captured in the A and B traps given the precision of measurement (Table 3). However, the POC flux recorded by the 550 and 800 m traps is lower than the flux captured by the 100 and 200 m floating traps (Table 4). There was relatively high variability in the POC export flux recorded by the floating traps, some of which is due to the relatively few number of deployments used to determine the average; eight deployments each only lasting 12–24 h were used to estimate mass fluxes at 100 and 200 m, compared with the 4-year flux time series recorded by the deep traps. Moreover, the floating trap deployments were not distributed evenly throughout the year; of the eight deployments, four occurred in April or May, two occurred in November, and one each occurred in December and June. Assuming a Martin function is a valid means of defining the change in POC flux with depth, we calculate a '*b*' value of 0.6 for the mean 100, 200, 550, and 800 m trap data summarized above. A trapping study by Nelson et al. (1987) in the same region

measured fluxes from traps deployed at 100, 300, and 500 m in May 1983, and these data yield a b value of 0.3. If we use our one May deployment from 2005, which captured POC fluxes two to ten times higher than any other floating trap deployment, we calculate a b value of 0.9.

POC fluxes through the upper part of the water column in this nearshore basin are very likely influenced by non-vertical transport processes; this may contribute to the low b values calculated from our flux data. However, below 500 m, the results here suggest that the path of particle sinking is more likely to be vertical. The similarity of C/Si ratios suggests very little degradation occurs between these depths, and hence b values must be low. If the uncertainty in POC flux to the deep traps is $\pm 10\%$ and if the fluxes of POC at 550 and 800 m agree to within 20%, this constrains the b value to something <0.6. All indications suggest that degradation of settling POC is attenuated relative to the open ocean in which b values are on average >0.8 (Berelson, 2001).

6. Conclusions

The data presented here describe a 4-year time series of particle flux measurements from San Pedro Basin. Four years of flux data for mass, non-biogenic detritus, POC, PON, $bSiO_2$, $CaCO_3$, $\delta^{13}C_{org}$, and $\delta^{15}N$ coupled with climatic records reveal:

(1) Sediment traps at 550 and 800 m record very similar timing and magnitude of the fluxes listed above. The mean (± 1 sdom) fluxes of mass, POC, $CaCO_3$, $bSiO_2$, and PON at 550 mm were 516 ± 42 mg/m^2 d, 3.18 ± 0.26 mmol C/m^2 d, 0.70 ± 0.05 mmol C/m^2 d, 1.31 ± 0.21 mmol bSi/m^2 d, and 0.35 ± 0.03 mmol N/m^2 d, respectively. The mean value of $\delta^{13}C_{org}$ in 550 m trap was -21.8 ± 0.2‰ and the average $\delta^{15}N$ of 550 m trap material was 8.9 ± 0.2‰. Traps at 800 m had similar fluxes and the same isotopic values (± 1 standard deviation). The measured ^{210}Pb fluxes into the two moored traps is quite similar to the inventory in bottom sediments, suggesting that the trap fluxes are not greatly different than the fluxes on time scales of several decades.

(2) The temporal coherence between fluxes captured by the 550 and 800 m traps implies a mean particle settling velocity of 83 m/d or greater, at least during high flux periods. The source of particle formation is probably patchy and may not be located directly above the trap mooring, however the similarity in the timing and magnitude of fluxes caught in the 550 and 800 m traps suggests that particle production must be evenly distributed around the trap location (accounting for mean advective influences) and/or particle settling below 550 m depth is essentially vertical.

(3) A comparison of the timing of rainfall events and detrital flux, $\delta^{13}C_{org}$, $\delta^{15}N$, and C_{org}/N indicates little significant correlation between rainfall and flux of terrestrially derived particulate matter to SPB. $\delta^{13}C_{org}$ values indicate that the primary organic carbon source to SPB floor sediments is marine phytoplankton. Floating traps located at 100 and 200 m during 24–48 h deployments in November, April, May, and June all capture detrital fluxes that are less than detrital fluxes captured in traps at 550 and 800 m. We propose that the rain-out from nepheloid layers and scavenging of lithogenic mineral grains by organic-rich sinking particles plays a role in generating the net detrital flux to the deep basin. POC export can occur with the aid of biogenic ballast and in the absence of much lithogenic ballast.

(4) Regional upwelling leads to near synchronicity between productivity and export. Satellite observations of chlorophyll a are temporally correlated with fluxes of POC; however chlorophyll a concentrations are a poor predictor of the quantity of POC falling at 550 m.

Acknowledgments

We would like to thank numerous contributors to the project including Tony Michaels, Michael Neumann, Will Beaumont, Tim Riedel, Liz Caporelli, Alice Alldredge, Carly Buchwald, Ronen Gersman, the Captains and crew of the R/V Sea Watch, Captain Kenny Kivett, Captain Dennis Dunn, and Jim Matsukas. We thank the three anonymous reviewers and DSR editor (D. Steinberg) whose comments were enormously helpful. We would like to thank NSF for its generous funding support to OCE-0351169 (to WMB and DEH) and NOAA Climate and Global Change postdoctoral fellowship support (to AK).

References

Altabet, M.A., Pilskaln, C., Thunell, R., Pride, C., Sigman, D., Chavez, F., Francois, R., 1999. The nitrogen isotope biogeochemistry of sinking particles from the margin of the Eastern North Pacific. Deep-Sea Research Part I: Oceanographic Research Papers 46 (4), 655–679.

Berelson, W.M., 1991. The flushing of two deep-sea basins, southern California borderland. Limnology and Oceanography 36 (6), 1150–1166.

Berelson, W.M., 2001. The flux of particulate organic carbon into the ocean interior: a comparison of four U.S. JGOFS Regional Studies. Oceanography 14, 4.

Bruland, K.W., Bertine, K., Koide, M., Goldberg, E.D., 1974. History of metal pollution in southern California coastal zone. Environmental Science and Technology 8 (5), 425–432.

Bruland, K.W., Franks, R.P., Landing, W.M., Soutar, A., 1981. Southern California inner basin sediment trap calibration. Earth and Planetary Science Letters 53 (3), 400–408.

Buesseler, K.O., 1991. Do upper-ocean sediment traps provide an accurate record of particle-flux. Nature 353 (6343), 420–423.

Buesseler, K.O., 1998. The decoupling of production and particulate export in the surface ocean. Global Biogeochemical Cycles 12 (2), 297–310.

Buesseler, K.O., Antia, A.N., Chen, M., Fowler, S.W., Gardner, W.D., Gustafsson, O., Harada, K., Michaels, A.F., van der Loeff'o, M.R., Sarin, M., Steinberg, D.K., Trull, T., 2007a. An assessment of the use of sediment traps for estimating upper ocean particle fluxes. Journal of Marine Research 65 (3), 345–416.

Buesseler, K.O., Lamborg, C.H., Boyd, P.W., Lam, P.J., Trull, T.W., Bidigare, R.R., Bishop, J.K.B., Casciotti, K.L., Dehairs, F., Elskens, M., Honda, M., Karl, D.M., Siegel, D.A., Silver, M.W., Steinberg, D.K., Valdes, J., Van Mooy, B., Wilson, S., 2007b. Revisiting carbon flux through the ocean's twilight zone. Science 316 (5824), 567–570.

Cheng, T., Hammond, D.E., Berelson, W.M., Hering, J.G., Dixit, S., 2009. Dissolution kinetics of biogenic silica collected from the water column and sediments of three southern California borderland basins. Marine Chemistry 113 (1–2), 41–49.

Collins, L., 2009. A sediment trap-based study of particle fluxes in San Pedro basin. Remineralization rates of organic carbon and biogenic silica. University of Southern California, Los Angeles, CA.

Crisp, P.T., Brenner, S., Venkatesan, M.I., Ruth, E., Kaplan, I.R., 1979. Organic-chemical characterization of sediment-trap particulates from San-Nicolas, Santa-Barbara, Santa-Monica and San-Pedro Basins, California. Geochimica et Cosmochimica Acta 43 (11), 1791–1801.

Degens, E.T., 1969. Biogeochemistry of stable carbon isotopes. In: Eglinton, G., Murphy, M.T.J. (Eds.), Organic Geochemistry, Methods and Results. Springer-Verlag, New York, pp. 304–328.

DeMaster, D.J., 1979. The Marine Budgets of Silica and ^{32}Si. Yale University, New Haven.

DeMaster, D.J., 1991. Measuring biogenic silica in sediments and suspended matter. American Geophysical Union.

Devol, A.H., Hartnett, H.E., 2001. Role of the oxygen-deficient zone in transfer of organic carbon to the deep ocean. Limnology and Oceanography 46 (7), 1684–1690.

Dong, C.M., McWilliams, J.C., 2007. A numerical study of island wakes in the Southern California Bight. Continental Shelf Research 27 (9), 1233–1248.

Drake, D.E., Gorsline, D.S., 1973. Distribution and transport of suspended particulate matter in Hueneme, Redondo, Newport, and La Jolla Submarine Canyons, California. Geological Society of America Bulletin 84 (12), 3949–3968.

Dymond, J., Fischer, K., Clauson, M., Cobler, R., Gardner, W., Richardson, M.J., Berger, W., Soutar, A., Dunbar, R., 1981. A sediment trap intercomparison study in the Santa-Barbara Basin. Earth and Planetary Science Letters 53 (3), 409–418.

Emery, K.O., 1960. The Sea Off Southern California: A Modern Habitat of Petroleum, New York. Wiley.

Fuhrman, J.A., Hewson, I., Schwalbach, M.S., Steele, J.A., Brown, M.V., Naeem, S., 2006. Annually reoccurring bacterial communities are predictable from ocean

conditions. Proceedings of the National Academy of Sciences of the United States of America 103 (35), 13104–13109.
Fukuda, R., Ogawa, H., Nagata, T., Koike, I., 1998. Direct determination of carbon and nitrogen contents of natural bacterial assemblages in marine environments. Applied and Environmental Microbiology 64 (9), 3352–3358.
Fuller, C., Hammond, D.E., 1983. The fallout rate of Pb-210 on the western coast of the United States. Geophysical Research Letters 10 (12), 1164–1167.
Gardner, W.D., 1980. Field assessment of sediment traps. Journal of Marine Research 38 (1), 41–52.
Gorsline, D.S., 1978. Anatomy of margin basins. Journal of Sedimentary Petrology 48, 4.
Hagadorn, J.W., Stott, L.D., Sinha, A., Rincon, M., 1995. Geochemical and sedimentologic variations in inter-annually laminate sediments from Santa Monica Basin. Marine Geology 125 (1–2), 111–131.
Harris, D., Horwarth, W., van Kessel, C., 2001. Acid fumigation of soils to remove carbonates prior to total organic carbon or carbon-13 isotopic analysis. Soil Science Society of America Journal 65 (6), 1853–1856.
Hastings, M.G., Sigman, D.M., Lipschultz, F., 2003. Isotopic evidence for source changes of nitrate in rain at Bermuda. Journal of Geophysical Research 108 (D24), 4790.
Hickey, B., 1991. Variability in two deep coastal basins (Santa Monica and San Pedro) off southern California. Journal of Geophysical Research 96 (C9), 16689–16708.
Hickey, B.M., 1992. Circulation over the Santa-Monica San-Pedro Basin and Shelf. Progress in Oceanography 30 (1-4), 37–115.
Hickey, B.M., Dobbins, E.L., Allen, S.E., 2003. Local and remote forcing of currents and temperature in the central Southern California Bight. Journal of Geophysical Research—Oceans 108 (C3).
Honjo, S., Doherty, K.W., 1988. Large aperture time-series sediment traps—design objectives, construction and application. Deep-Sea Research Part A–Oceanographic Research Papers 35 (1), 133–149.
Honjo, S., Manganini, S.J., Krishfield, R.A., Francois, R., 2008. Particulate organic carbon fluxes to the ocean interior and factors controlling the biological pump: a synthesis of global sediment trap programs since 1983. Progress in Oceanography 76 (3), 217–285.
Huh, C.A., Beasley, T.M., 1987. Profiles of dissolved and particulate thorium isotopes in the water column of coastal southern California. Earth and Planetary Science Letters 85 (1–3), 1–10.
Huh, C.A., Ku, T.L., Luo, S.D., Landry, M.R., Williams, P.M., 1993. Fluxes of Th isotopes in the Santa-Monica Basin, Offshore California. Earth and Planetary Science Letters 116 (1–4), 155–164.
Huh, C.A., Small, L.F., Niemnil, S., Finney, B.P., Hickey, B.M., Kachel, N.B., Gorsline, D.S., Williams, P.M., 1990. Sedimentation dynamics in the Santa-Monica San-Pedro Basin off Los-Angeles—radiochemical, sediment trap and transmissometer studies. Continental Shelf Research 10 (2), 137–164.
Kepner, R.L., Pratt, J.R., 1994. Use of fluorochromes for direct enumeration of total bacteria in environmental samples—past and present. Microbiological Reviews 58 (4), 603–615.
Knap, A.H., 1994. JGOFS sediment trap methods. In: Knap, A.H. (Ed.), IOC Manuals and Guides. Intergovernmental Oceanographic Commission, pp. 180.
Knapp, A.N., Hastings, M.G., Sigman, D.M., Lipschultz, F., Galloway, J.N., 2010. The flux and isotopic composition of reduced and total nitrogen in Bermuda rain. Marine Chemistry 120 (1–4), 83–89.
Lohrenz, S.E., Knauer, G.A., Asper, V.L., Tuel, M., Michaels, A.F., Knap, A.H., 1992. Seasonal variability in primary production and particle flux in the northwestern Sargasso Sea: U.S. JGOFS Bermuda Atlantic time-series study. Deep-Sea Research Part A—Oceanographic Research Papers 39 (7-8), 1373–1391.
Liu, K.-K., Kaplan, I.R., 1989. The eastern tropical Pacific as a source of [15]N-enriched nitrate in seawater off southern California. Limnology and Oceanography 34, 820–830.
Martin, J.H., Knauer, G.A., Karl, D.M., Broenkow, W.W., 1987. Vertex—carbon cycling in the northeast Pacific. Deep-Sea Research Part A—Oceanographic Research Papers 34 (2), 267–285.
Moore, W.S., Bruland, K.W., Michel, J., 1981. Fluxes of uranium and thorium series isotopes in the Santa-Barbara basin. Earth and Planetary Science Letters 53 (3), 391–399.
Mortlock, R.A., Froelich, P.N., 1989. A simple method for the rapid determination of biogenic opal in pelagic marine sediments. Deep-Sea Research Part A—Oceanographic Research Papers 36 (9), 1415–1426.
Muller-Karger, F.E., Varela, R., Thunell, R., Luerssen, R., Hu, C.M., Walsh, J.J., 2005. The importance of continental margins in the global carbon cycle. Geophysical Research Letters 32, 1.
Nardin, T.R., 1981. Seismic-stratigraphy of Santa Monica basin fill, southern California borderland. AAPG Bulletin—American Association of Petroleum Geologists 65 (5), 964.
Nelson, J.R., Beers, J.R., Eppley, R.W., Jackson, G.A., Mccarthy, J.J., Soutar, A., 1987. A particle-flux study in the Santa-Monica San-Pedro Basin off Los-Angeles—particle-flux, primary production, and transmissometer survey. Continental Shelf Research 7 (3), 307–328.
Nezlin, N.P., DiGiacomo, P.M., 2005. Satellite ocean color observations of stormwater runoff plumes along the San Pedro Shelf (southern California) during 1997–2003. Continental Shelf Research 25 (14), 1692–1711.
Nezlin, N.P., DiGiacomo, P.M., Stein, E.D., Ackerman, D., 2005. Stormwater runoff plumes observed by SeaWiFS radiometer in the Southern California Bight. Remote Sensing of Environment 98 (4), 494–510.
Passow, U., Shipe, R.F., Murray, A., Pak, D.K., Brzezinski, M.A., Alldredge, A.L., 2001. The origin of transparent exopolymer particles (TEP) and their role in the sedimentation of particulate matter. Continental Shelf Research 21 (4), 327–346.
Perdue, E.M., Koprivnjak, J.-F., 2007. Using the C/N ratio to estimate terrigenous inputs of organic matter to aquatic environments. Estuarine, Coastal and Shelf Science 73 (1–2), 65–72.
Primeau, F., 2006. On the variability of the exponent in the power law depth dependence of POC flux estimated from sediment traps. Deep-Sea Research Part I—Oceanographic Research Papers 53 (8), 1335–1343.
Reimers, C.E., Jahnke, R.A., McCorkle, D.C., 1992. Carbon fluxes and burial rates over the continental slope and rise off Central California with implications for the global carbon cycle. Global Biogeochemical Cycles, 6.
Sautter, L.R., Thunell, R.C., 1991. Planktonic foraminiferal response to upwelling and seasonal hydrographic conditions—sediment trap results from San-Pedro-Basin, Southern California Bight. Journal of Foraminiferal Research 21 (4), 347–363.
Schnetzer, A., Miller, P.E., Schaffner, R.A., Stauffer, B.A., Jones, B.H., Weisberg, S.B., DiGiacomo, P.M., Berelson, W.M., Caron, D.A., 2007. Blooms of pseudo-nitzschia and domoic acid in the San Pedro Channel and Los Angeles harbor areas of the Southern California Bight, 2003–2004. Harmful Algae 6 (3), 372–387.
Schwalbach, J.R., 1982. A sediment budget for the northern region of the California continental borderland. University of Southern California, Los Angeles, p. 212.
Schwalbach, J.R., Gorsline, D.S., 1985. Holocene sediment budgets for the basins of the California Continental Borderland. Journal of Sedimentary Petrology 55 (6), 829–842.
Sekula-Wood, E., Schnetzer, A., Benitez-Nelson, C.R., Anderson, C., Berelson, W.M., Brzezinski, M.A., Burns, J.M., Caron, D.A., Cetinic, I., Ferry, J.L., Fitzpatrick, E., Jones, B.H., Miller, P.E., Morton, S.L., Schaffner, R.A., Siegel, D.A., Thunell, R., 2009. Rapid downward transport of the neurotoxin domoic acid in coastal waters. Nature Geoscience 2 (4), 272–275.
Shipe, R.F., Brzezinski, M.A., 2001. A time series study of silica production and flux in an eastern boundary region: Santa Barbara Basin, California. Global Biogeochemical Cycles 15 (2), 517–531.
Shipe, R.F., Passow, U., Brzezinski, M.A., Graham, W.M., Pak, D.K., Siegel, D.A., Alldredge, A.L., 2002. Effects of the 1997–98 El Nino on seasonal variations in suspended and sinking particles in the Santa Barbara basin. Progress in Oceanography 54 (1–4), 105–127.
Soutar, A., Kling, S.A., Crill, P.A., Duffrin, E., Bruland, K.W., 1977. Monitoring the marine environment through sedimentation. Nature 266 (5598), 136–139.
Strickland, J.P.T., 1968. A Practical Handbook of Seawater Analysis. Fisheries Research Board of Canada, Halifax.
Thunell, R., Benitez-Nelson, C., Varela, R., Astor, Y., Muller-Karger, F., 2007. Particulate organic carbon fluxes along upwelling-dominated continental margins: rates and mechanisms. Global Biogeochemical Cycles 21 (1).
Thunell, R., Tappa, E., Pride, C., Kincaid, E., 1999. Sea-surface temperature anomalies associated with the 1997–1998 El Nino recorded in the oxygen isotope composition of planktonic foraminifera. Geology 27 (9), 843–846.
Thunell, R.C., 1998. Particle fluxes in a coastal upwelling zone: sediment trap results from Santa Barbara Basin, California. Deep-Sea Research Part II—Topical Studies in Oceanography 45 (8–9), 1863–1884.
Thunell, R.C., Moore, W.S., Dymond, J., Pilskaln, C.H., 1994a. Elemental and isotopic fluxes in the Southern California Bight—a time-series sediment trap study in the San-Pedro basin. Journal of Geophysical Research—Oceans 99 (C1), 875–889.
Thunell, R.C., Pilskaln, C.H., Tappa, E., Sautter, L.R., 1994b. Temporal variability in sediment fluxes in the San-Pedro Basin, Southern California Bight. Continental Shelf Research 14 (4), 333–352.
Turley, C.M., Hughes, D.J., 1992. Effects of storage on direct estimates of bacterial numbers of preserved seawater samples. Deep-Sea Research Part A—Oceanographic Research Papers 39 (3–4A), 375–394.
Turley, C.M., Mackie, P.J., 1995. Bacterial and cyanobacterial flux to the deep NE Atlantic on sedimenting particles. Deep-Sea Research Part I—Oceanographic Research Papers 42 (8), 1453–1474.
Vanucci, S., Dell'Anno, A., Pusceddu, A., Fabiano, M., Lampitt, R.S., Danovaro, R., 2001. Microbial assemblages associated with sinking particles in the Porcupine Abyssal Plain (NE Atlantic Ocean). Progress in Oceanography 50 (1–4), 105–121.
Vrede, K., Heldal, M., Norland, S., Bratbak, G., 2002. Elemental composition (C, N, P) and cell volume of exponentially growing and nutrient-limited bacterioplankton. Applied and Environmental Microbiology 68 (6), 2965–2971.
Warrick, J., Mertes, L.K., Washburn, L., Siegel, D., 2004. Dispersal forcing of southern California river plumes, based on field and remote sensing observations. Geo-Marine Letters 24 (1), 46–52.
Wickham, J.D., 1975. Observations of the California countercurrent. Journal of Marine Research 33 (3), 325–340.
Wooster, W.S., Reid, J.L., 1963. Eastern boundary currents. In: Hill, M.N. (Ed.), The Sea. Interscience Publishers, New York, pp. 253–280.
Ziveri, P., Thunell, R.C., Rio, D., 1994. Export production of coccolithophores in an upwelling region—results from San-Pedro Basin, southern California borderlands. Marine Micropaleontology 24 (3–4), 335–358.